การสังเคราะห์เอทิล เทอร์เชียรีบิวทิล อีเทอร์ จากเอทานอลและเทอร์เชียรี บิวทานอลโดยใช้ตัวเร่งปฏิกิริยาซีโอไลต์เบตา ในเครื่องปฏิกรณ์แบบเพอร์เวเพอเรทีฟเมมเบรน

นายวรพล เกียรติกิตติพงษ์

วิทยานิพนธ์นี้เป็นส่วนหนึ่งของการศึกษาตามหลักสูตรปริญญาวิศวกรรมศาสตรมหาบัณฑิต
สาขาวิชาวิศวกรรมเคมี ภาควิชาวิศวกรรมเคมี
คณะวิศวกรรมศาสตร์ จุฬาลงกรณ์มหาวิทยาลัย
ปีการศึกษา 2544

ISBN 974-03-0333-1

SYNTHESIS OF ETHYL TERTIARY BUTYL ETHER FROM ETHANOL AND TERTIARY BUTANOL USING BETA ZEOLITE CATALYST IN A PERVAPORATIVE MEMBRANE REACTOR

Mr. Worapon Kiatkittipong

A Thesis Submitted in Partial Fulfillment of the Requirements
for the Degree of Master of Engineering in Chemical Engineering
Department of Chemical Engineering
Faculty of Engineering
Chulalongkorn University
Academic Year 2001

ISBN 974-03-0333-1

Thesis Title	Synthesis of Ethyl Tertiary Butyl Ether from Ethanol and Tertiary Butanol Using Beta Zeolite Catalyst in a Pervaporative Membrane Reactor
By	Mr. Worapon Kiatkittipong
Field of Study	Chemical Engineering
Thesis Advisor	Assistant Professor Suttichai Assabumrungrat, Ph.D.
Thesis Co-advisor	Professor Piyasan Praserthdam, Dr.Ing.

Accepted by the Faculty of Engineering, Chulalongkorn University in Partial Fulfillment of the Requirements for the Master 's Degree

…….. Dean of Faculty of Engineering
(Professor Somsak Panyakeow, Dr.Eng.)

THESIS COMMITTEE

…….. Chairman
(Associate Professor Tawatchai Charinpanitkul, Dr.Ing)

……. Thesis Advisor
(Assistant Professor Suttichai Assabumrungrat, Ph.D.)

…….. Thesis Co-advisor
(Professor Piyasan Praserthdam, Dr.Ing.)

…….. Member
(Assistant Professor Prasert Pavasant, Ph.D.)

วรพล เกียรติกิตติพงษ์ : การสังเคราะห์เอทิล เทอร์เชียรีบิวทิล อีเทอร์จากเอทานอลและเทอร์เชียรี บิวทานอลโดยใช้ตัวเร่งปฏิกิริยาซีโอไลต์เบตา ในเครื่องปฏิกรณ์แบบเพอร์เวเพอเรทีฟเมมเบรน. (SYNTHESIS OF ETHYL TERTIARY BUTYL ETHER FROM ETHANOL AND TERTIARY BUTANOL USING BETA ZEOLITE CATALYST IN A PERVAPORATIVE MEMBRANE REACTOR) อ.ที่ปรึกษา : ผศ.ดร.สุทธิชัย อัสสะบำรุงรัตน์, อ.ที่ปรึกษาร่วม : ศ.ดร.ปิยะสาร ประเสริฐธรรม 73 หน้า. ISBN 974-03-0333-1.

การศึกษาปฏิกิริยาการสังเคราะห์เอทิล เทอร์เชียรีบิวทิล อีเทอร์ในวัฏภาคของเหลวจากเอทานอลและเทอร์เชียรีบิวทิล แอลกอฮอล์ แบ่งได้เป็น 3 ส่วนหลักคือ การศึกษาจลนพลศาสตร์ของตัวเร่งปฏิกิริยาซีโอไลต์เบตาบนตัวรองรับ การศึกษาการแพร่ผ่านเยื่อแผ่นชนิดโพลีไวนิลแอลกอฮอล์และการศึกษาในเครื่องปฏิกรณ์แบบเพอร์เวเพอเรทีฟเมมเบรน ตัวเร่งปฏิกิริยาที่เลือกใช้คือตัวเร่งปฏิกิริยาซีโอไลต์เบตาบนตัวรองรับ เนื่องจากมีประสิทธิผลดีกว่าตัวเร่งปฏิกิริยาแอมเบอร์ลิซ 15 การศึกษาจลนพลศาสตร์กระทำในเครื่องปฏิกรณ์ซึ่งดำเนินการแบบกึ่งกะ ศึกษาผลของการถ่ายเทมวลสารภายนอกโดยการเปลี่ยนค่าความเร็วรอบในการกวน และทำการศึกษาที่อุณหภูมิเท่ากับ 323 333 และ 343 เคลวิน เพื่อหาค่าตัวแปรในสมการของอาร์เรเนียสและแวนท์ฮอฟ พบว่าแบบจำลองทั้งที่อธิบายในรูปของความเข้มข้นและในรูปแอคติวิตีสามารถทำนายผลการทดลองได้ดี การศึกษาการแพร่ผ่านของระบบน้ำ-แอลกอฮอล์ พบว่าเยื่อแผ่นมีประสิทธิภาพในการดึงน้ำออกที่ความเข้มข้นของน้ำไม่เกิน 62%โดยโมล ส่วนในการศึกษาการแพร่ผ่านของระบบสารผสมทั้ง 4 ชนิดได้แก่ เอทานอล เทอร์เชียรีบิวทิล แอลกอฮอล์ เอทิล เทอร์เชียรีบิวทิล อีเทอร์และน้ำ ที่ 3 อุณหภูมิได้แก่ 323 333 และ 343 เคลวิน พบว่าเยื่อแผ่นให้การเลือกผ่านน้ำได้มากที่สุด โดยค่าสัมประสิทธิ์ของการแพร่เป็นไปตามสมการของอาร์เรเนียสเช่นกัน สำหรับการศึกษาในเครื่องปฏิกรณ์แบบเพอร์เวเพอเรทีฟเมมเบรนนั้นได้ทำการศึกษาทั้งการทำการทดลองและการสร้างแบบจำลองทางคณิตศาสตร์ แบบจำลองทางคณิตศาสตร์ซึ่งอธิบายในรูปแอคติวิตีโดยค่าตัวแปรต่างๆได้จากการทดลองซึ่งเป็นอิสระต่อกัน ถูกนำมาใช้อธิบายถึงประสิทธิภาพของเครื่องปฏิกรณ์แบบเพอร์เวเพอเรทีฟเมมเบรน โดยผลที่ได้จากแบบจำลองทางคณิตศาสตร์สอดคล้องกับผลการทดลองเป็นอย่างดี และพบว่าค่าอัตราส่วนระหว่างจำนวนโมลตั้งต้นของเอทานอลต่อเทอร์เชียรีบิวทิล แอลกอฮอล์ อัตราส่วนระหว่างพื้นที่ของเยื่อแผ่นต่อโมลตั้งต้นของเทอร์เชียรีบิวทิล แอลกอฮอล์ อัตราส่วนระหว่างปริมาณตัวเร่งปฏิกิริยาต่อโมลตั้งต้นของเทอร์เชียรีบิวทิล แอลกอฮอล์ และอุณหภูมิในการดำเนินการ มีผลอย่างมากต่อประสิทธิผลของเครื่องปฏิกรณ์ โดยค่าอัตราส่วนระหว่างพื้นที่ของเยื่อแผ่นต่อโมลตั้งต้นของเทอร์เชียรีบิวทิล แอลกอฮอล์ และอุณหภูมิในการดำเนินการมีค่าที่เหมาะสมเนื่องจากการแข่งขันกันของอัตราการเกิดปฏิกิริยา และการสูญเสียไปของสารตั้งต้น

ภาควิชา.....วิศวกรรมเคมี..... ลายมือชื่อนิสิต.....

สาขาวิชา.....วิศวกรรมเคมี..... ลายมือชื่ออาจารย์ที่ปรึกษา.....

ปีการศึกษา.....2544..... ลายมือชื่ออาจารย์ที่ปรึกษาร่วม.....

#4270517051 : MAJOR CHEMICAL ENGINEERING

KEYWORD: PERVAPORATION / PERVAPORATIVE MEMBRANE REACTOR / ETBE SYNTHESIS / KINETICS / ACTIVITY COEFFICIENT

WORAPON KIATKITTIPONG : SYNTHESIS OF ETHYL TERTIARY BUTYL ETHER FROM ETHANOL AND TERTIARY BUTANOL USING BETA ZEOLITE CATALYST IN A PERVAPORATIVE MEMBRANE REACTOR.
THESIS ADVISOR : ASSIST.PROF. SUTTICHAI ASSABUMRUNGRAT, Ph.D.,THESIS CO-ADVISOR : PROF. PIYASAN PRASERTHDAM, Dr.Ing., 73 pp. ISBN 974-03-0333-1.

A pervaporative membrane reactor for the synthesis of ethyl *tert*-butyl ether (ETBE) from a liquid phase reaction between ethanol (EtOH) and *tert*-butyl alcohol (TBA) was investigated. The study was divided into 3 main parts: kinetic study of supported β-zeolite, study on permeation through polyvinyl alcohol (PVA) membrane and study on pervaporative membrane reactor. The supported β-zeolite was selected because of better performance compared to a commercial catalyst, Amberlyst-15. The kinetic study was carried out using a semi-batch reactor. The effect of external mass transfer was investigated by varying stirring speeds. Three temperature levels of 323, 333 and 343 K were performed in the study to obtain the parameters in the Arrhenius' equation and the Van't Hoff equation. Both concentration-based and activity-based models can fit the experimental results well. The permeation studies of H_2O-EtOH binary system revealed that the membrane worked effectively for H_2O removal at the mixtures containing H_2O content lower than 62mol%. The permeation studies of quaternary mixtures (H_2O-EtOH-TBA-ETBE) were performed at 3 temperature levels of 323, 333 and 343 K. It was found that the membrane was preferentially permeable to H_2O. The permeability coefficients were correlated with the Arrhenius' equation. In the pervaporative membrane reactor studies, both experiment and simulation were carried out. An activity-based model was developed to investigate the performance of the pervaporative membrane reactor using parameters obtained from the independent experiments. Simulation results agreed well with experimental results. It was observed that the ratio of initial mole of EtOH to TBA, the ratio of membrane area to initial mole of TBA, the ratio of the amount of catalyst to initial mole of TBA and the operating temperature played important roles on the reactor performance. The analysis of the operating temperature and the ratio of membrane area to initial mole of TBA showed an optimum yield due to the competing effect of rate of reaction and rate of reactant losses.

Department…Chemical Engineering……	Student's signature……..
Field of study….Chemical Engineering…	Advisor's signature…….
Acadamic year……..2001……..…..	Co-advisor's signature……..…...

ACKNOWLEDGEMENTS

The author would like to express his highest gratitude to Assistant Professor Suttichai Assabumrungrat and Professor Piyasan Praserthdam for their inspiration, guidance, and supervision throughout this research study. In addition, he is also grateful to Associate Professor Tawatchai Charinpanitkul, as the chairman, and Assistant Professor Prasert Pavasant, as a member of the thesis committee.

Thank you for the financial support from Thailand Research Fund, TJTTP-OECF and Graduate school, Chulalongkorn University.

Most of all, the author would like to express his highest gratitude to his parents who have always been the source of his support and encouragement.

Finally, grateful thanks to petrochemical laboratory members who have encouraged him over the years of his study.

CONTENTS

page

page

page

LIST OF TABLES

TABLE **page**

LIST OF FIGURES

FIGURE **page**

FIGURE **page**

Nomenclature

a_i	activity of species *i*	[-]
A	membrane area	[m^2]
c_i	concentration of species *i*	[mol/m^3]
F_i	correction factor of species *i*	[-]
k_{1a}	reaction rate constant of reaction (5.1)	
	in the activity-based model	[mol/(kg.s)]
k_{1c}	reaction rate constant of reaction (5.1)	
	in the concentration-based model	[m^6/(mol.kg.s)]
k_{2a}	reaction rate constant of reaction (5.2)	
	in the activity-based model	[mol/(kg.s)]
k_{2c}	reaction rate constant of reaction (5.2)	
	in the concentration-based model	[m^3/(kg.s)]
K_{1a}	equilibrium constant of reaction (5.1)	
	in the activity-based model	[-]
K_{1c}	equilibrium constant of reaction (5.1)	
	in the concentration-based model	[-]
K_{Wa}	water inhibition parameter	
	in the activity-based model	[-]
K_{Wc}	water inhibition parameter	
	in the concentration-based model	[m^3/mol]
m_i	number of mole of species *i*	[mol]
n_i	permeation rate of species *i*	[mol/s]
P_i	permeability coefficient of species *i*	[mol/(m^2.s)]
R_g	gas constant (=8.314 J/mol)	[J/mol]
r_j	reaction rate of reaction *j*	[mol/(kg.s)]
t	reaction time	[s]
T	temperature	[K]
W	catalyst weight	[kg]

x_i	mole fraction of species *i* in liquid mixture	[-]

Greek letter

γ_i	activity coefficient of species *i*	[-]
α	ratio of initial mole of EtOH to TBA	[-]
δ	ratio of membrane area to initial mole of TBA	[m^2/mol]
ϕ	ratio of the amount of catalyst to initial mole of TBA	[g/mol]
Θ	area of peek	[-]

Subscript

i	species *i*
j	reaction *j*
ETBE	ethyl *tert*-butyl ether
EtOH	ethanol
H_2O	water
MTBE	methyl *tert*-butyl ether
TBA	*tert*-butyl alcohol
o	initial value at $t = 0$
total	total mole

CHAPTER I
INTRODUCTION

Since lead compounds are being eliminated from fuels for reasons of public health and of environmental protection, oxygenates are gaining importance as gasoline blending components, not only as gasoline extenders and as octane enhancer but also as key ingredients for reducing the emissions of CO and VOCs (volatile organic compound). The U.S. Clean Air Act Amendments of 1990 increased the severity of the emission limits of vehicles and required the manufacture of clean fuel, including reformulated and oxygenated gasoline. The specification for reformulated gasoline must contain 2.7 wt% oxygen during the winter in the CO nonattainment areas of the United States.

The two main classes of competing oxygenates at present are alcohols and ethers, both possessing the desired characteristics of octane enhancement and CO emission reduction. In general, ethers are preferred over alcohols because of their fungibility, or blending characteristic, as they are more like conventional gasoline hydrocarbon constituents. Alcohols are substantially more polar than ethers and other gasoline hydrocarbons and, consequently, can result in phase separation in the presence of any water in the gasoline distribution system. Further, in spite of their low individual vapor pressure, the alcohols tend to produce a higher blending Reid vapor pressure (bRvp) and, thus, more volatile organic compound emissions.

Methyl *tert*-butyl ether (MTBE) synthesized commercially by the exothermic liquid phase reactor of methanol and isobutylene over an acid ion exchange resin catalyst was introduced as gasoline additives in 1979 and are currently the most frequently used gasoline additive. However the price of methanol mostly derived from natural gas goes up and recently, the investigation revealed that it has tendency to pollute underground water. As a result, there is pending legistation in a number of states in the U.S. banning MTBE (Parkinson, 1999).

Tert-amyl methyl ether (TAME) and *tert*-amyl ethyl ether (TAEE) were synthesized from *tert*-amyl alcohol (TAA) and methanol or ethanol, respectively. Although TAME and TAEE have better characteristic than MTBE such as lower bRvp, TAA is relatively expensive and, hence, it is less attractive to produce them.

Ethyl *tert*-butyl ether (ETBE) which is the major component of our interest may be a good alternative because, from the viewpoint of environmental protection, ETBE is derived from ethanol (EtOH) which can be obtained from renewable resources like biomass (Quitain *et al*.,1999). It is expected in France that 5% of fuel used in transportation should be produced from renewable energy by 2005 (Poitrate, 1999). In addition, ETBE has lower bRvp (4 psi) than MTBE (8-10 psi), which allows ETBE to be used successfully in obtaining gasoline with less bRvp than 7.8 psi as required in some hot places during summer (Cunill *et al*., 1993). A review on oxygenate fuels - market expansion and catalytic aspect of synthesis was given by Ancilloti and Fattoro (1998).

Since the synthesis of tertiary ethers is a typical example of equilibrium-limited reaction that produces by-product H_2O, the presence of H_2O has a strong inhibition effect on the catalytic activity (Cunill *et al*., 1993) and the conversion is generally low due to limits imposed by thermodynamic equilibrium. A combined process of separation and chemical reaction in a single unit operation which is one type of multifunctional reactors has attracted much attention for overcoming the equilibrium conversion. For this type of reaction, it is customary to remove H_2O from the reaction system because it does not only shift the forward reaction but also suppress water inhibition effect found in many catalysts. There are a number of processes proposed to improve ether yield, for examples, reactive distillation, reactive distillation with an external pervaporation unit and pervaporative membrane reactor. However, the pervaporative membrane reactor is a relatively new process and has drawn a number of attention from researchers in recent years.

From the above reasons, this research focused on the use of pervaporative membrane reactor to improve the yield of ETBE. The objectives of the study were to investigate

1. the performance of β-zeolite compared with the commercial Amberlyst-15 for the synthesis of ETBE from EtOH and TBA;
2. the kinetics of the reaction catalyzed by β-zeolite;
3. the permeation of H_2O, EtOH, TBA and ETBE through a polyvinyl alcohol membrane;
4. pervaporative membrane reactor performance both from experiment and mathematical simulation;
5. the effect of operating conditions such as temperature, feed molar composition, amount of catalyst and the ratio of membrane area to mass of feed mixture.

CHAPTER II

THEORY

This chapter provides some background information necessary for understanding the synthesis of ethyl *tert*-butyl ether (ETBE) from ethanol (EtOH) and *tert*-butyl alcohol (TBA) by β-zeolite in a pervaporative membrane reactor. The details on membrane definition, membrane reactor, pervaporation process, pervaporative membrane reactor, β-zeolite catalyst and supported catalyst for the pervaporative membrane reactor are provided in the following sections.

2.1 Membrane definition

A membrane is an interface between two bulk phases. It controls the exchange of mass with differing chemical and physical properties between them. The membrane phase can be one or a combination of the followings: a nonporous solid, microporous or macroporous solid with a fluid in the pores, a liquid phases with or without a second phase. Exchange between the two bulk phases across the membrane is caused from the presence of a driving force. The most common ones are chemical potential, such as pressure and concentration gradients, and electrical potential.

2.2 Membrane reactor

Membrane reactor offers the advantage over conventional reactors of combining separation and chemical reaction into a single unit. Membrane reactor can be classified into two types, i.e. inert membrane reactor and catalytically active membrane reactor. For the inert membrane reactor, membrane provides a medium for separation of product(s) formed within the catalyst pellets. For the catalytically active membrane, the catalyst is attached to the membrane surface or membrane pores. This membrane is inherently catalytically active. Catalysts can be contained in the membrane pores or on the membrane surface by several impregnation and adsorption techniques commonly used for conventional catalyst preparation. Therefore, the membranes serve as both a separator and a catalyst.

The major advantages of membrane reactor are for improving reactor performance, energy management and reducing intensity of operating condition. The following sections provide details of the membrane reactor by dividing into 2 subsections according to the types of applications of the membrane reactor.

2.2.1 Yield-enhancement of equilibrium-limited reactions

The most common application opportunity of membrane reactor lies in the circumvention of a chemical equilibrium so as to achieve higher per-pass conversions by selective permeation, through the membrane, of at least one of the reaction products. Most often are the removal of hydrogen in dehydrogenation reactions and the removal of water in esterification or etherification as shown in Figure 2.1a. Product removal may be selective (i.e., H_2 permeation through a composite Pd-ceramic membrane), or preferential (i.e., preferential permeation of H_2O than alcohol).

Equilibrium displacement can be enhanced through reaction coupling. Figure 2.1b shows the coupling of reactions at the opposite side of the membrane. In this case, on both sides of the membrane complementary processes are run using either the permeated species (chemical coupling, e.g., dehydrogenation/hydrogenation, or dehydrogenation/combustion reactions), or the heat generated in the reaction (thermal coupling, exothermic/endothermic processes). The reactions often use different catalysts, which would be packed on opposite sides of the membrane tube.

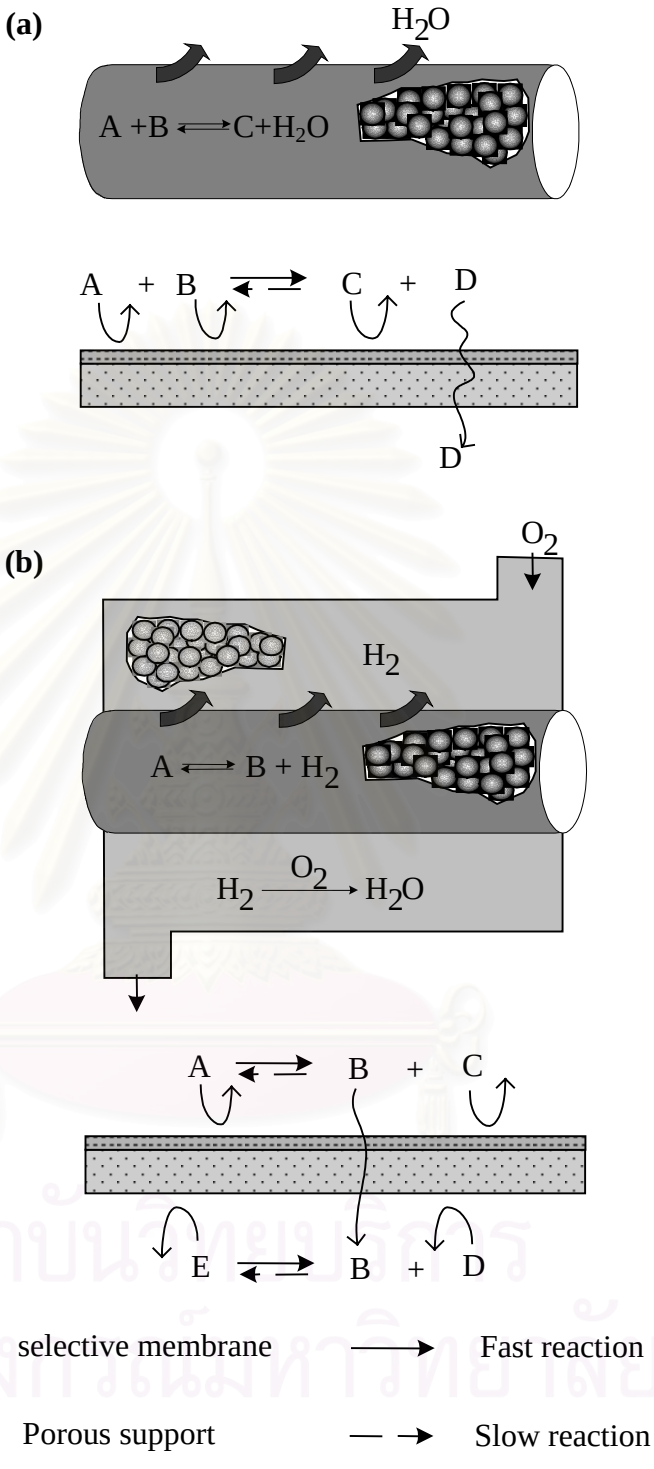

Figure 2.1 Application opportunities of inorganic membrane reactor (yield enhancement): (a) selective permeation of a reaction product of an equilibrium limited reaction; (b) coupling of reactions.

2.2.2 Selectivity enhancement

The improvement of reaction selectivity is a second field of application of membrane reactors on which most attention of the scientific community is nowadays addressed. In this context, considering consecutive reaction pathways, a permselective membrane could allow permeation of an intermediate product while rejecting either reactants or other undesired products (Figure 2.2a). As a result, subsequent reactions which consume the intermediate product can be suppressed. However, intermediate products (e.g. partially oxidized hydrocarbons) are larger than the complete reaction products (e.g. CO_2) or the reactants themselves (e.g. O_2). This requires the imaginative use of some unconventional permeation mechanisms (e.g. capillary condensation, surface diffusion or multi-layer diffusion), which is rather complex and strongly depends on the particular reaction and membrane considered.

Another way to increase selectivity is controlled addition of a reactant along the reactor, through either a permselective or a non-permselective membrane as showed in Figure 2.2b. In the recent year, the increasing of research is in this field because the membrane permselectivity is a less urgent need (if any) for this kind of applications. The permeation of reactant (e.g. O_2, H_2) through membrane to the reaction zone is control the partial pressure in the reaction zone to low that is increase the selectivity of intermediate product. Examples of reaction in this case are partial oxidation, oxidative coupling and oxidative dehydrogenation.

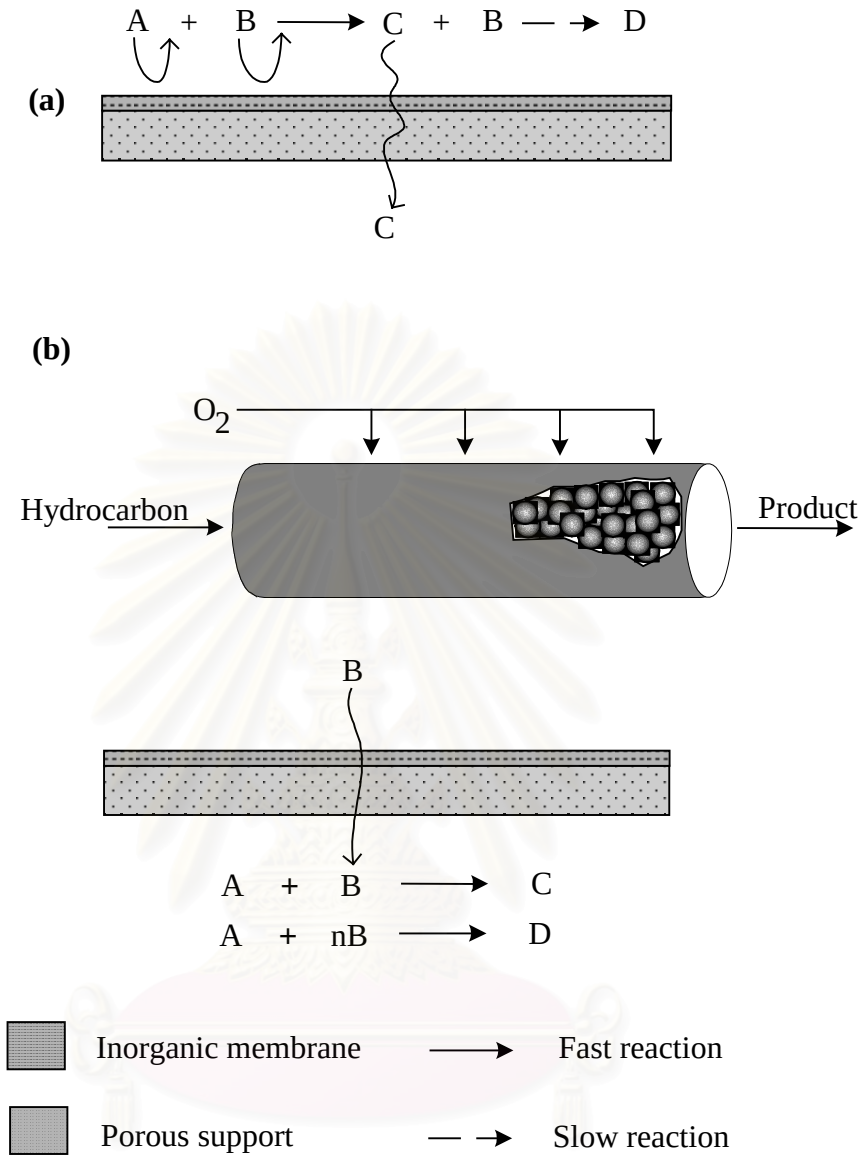

Figure 2.2 Application opportunities of inorganic membrane reactor (selectivity enhancement): (a) selective permeation of an intermediate, desired product; (b) dosing a reactant through the membrane.

2.3 Pervaporation process

Pervaporation is one of important membrane separation processes. It enables the separation of a liquid mixture with close boiling points, azeotropic mixtures, isomers, and mixtures consisting of heat-sensitive compounds by partly vaporizing it through a dense membrane. The transport mechanism can be described by the solution diffusion model involving 3 main steps of 1) sorption of liquid into the membrane at the feed side 2) transport through the membrane and 3) desorption into the vapor phrase at the permeate side of the membrane (Lee and Hong, 1997; Sentarh *et al*.,1998).

The liquid mixture is in contact with the upstream side of the membrane and the product permeating through the polymeric membrane is removed as a vapor at the downstream side by creating a low partial pressure. Figure 2.3 shows a schematic diagram of a typical pervaporation system. It comprises a pervaporation module, a condenser, and a vacuum pump.

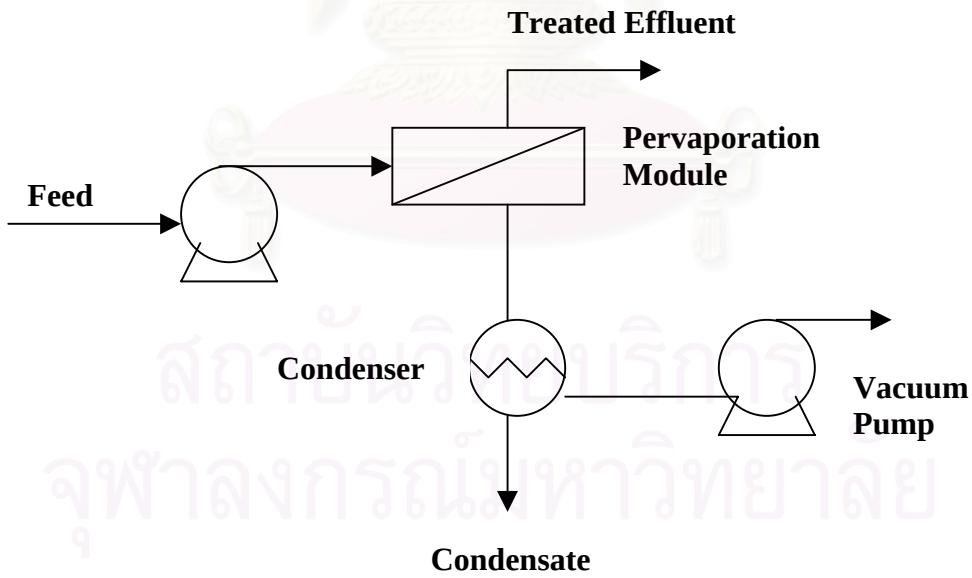

Figure 2.3 Schematic of a typical pervaporation system.

The separation of liquid mixtures by using pervaporation method can be classified into three fields;

1) dehydration of water/organic solvents
2) removal of organic solvent for aqeous solutions and
3) separation of organic/organic solvent mixtures.

The performance of the pervaporation process depends not only upon the physicochemical properties of the polymeric materials and the structure of membrane but also upon the operating conditions, e.g. temperature, downstream pressure and composition of mixture. The followings summarize the effects of various factors on the performance of the pervaporation process.

1. Physico-chemical properties.

The permeation of solvents through a non-porous membrane usually can be described in terms of sorption and molecular diffusion. The extent of sorption (also called swelling) as well as the sorption selectivity are therefore determined by chemical nature of polymer and that of the solvents.

2. Feed composition.

A change in feed composition directly affects the sorption phenomena at the liquid-membrane interface. The sorption selectivity depends obviously on the power of interaction between components. The extent of swelling as well as the sorption selectivity depends on the structure of polymer network. The lower affinity to the membrane can penetrate into the swollen system, and contribute to better swelling.

3. Feed concentration

According to Fick's law, the permeation is proportional to the activity gradient across the membrane. Since the feed concentration directly affects the membrane activity, the increased feed concentration increases the driving force and the permeation flux through the membrane.

4. Operating temperature

The variation of permeation rate follows from the operating temperature can be correlated with the Arrhenius' equation.

$$J_p = J_0 \exp(-E_p / R_g T) \qquad (2.1)$$

where J_P is the permeation rate, J_0 is the pre-exponential factor, E_p is the apparent activation energy of permeation, and R_g and T are the gas constant and temperature, respectively.

5. Downstream pressure

Pervaporation process controls downstream pressure by pumping the permeate from downstream interface in the vapor form to provide the driving force. The decreased vapor pressure in downstream compartment is equivalent to an increased driving force for component transportation.

The values of partial vapor pressure, which directly control the transport of solvents, result from a dynamic equilibrium between the transport flux of the permeates and the pumping rate.

2.4 Pervaporative membrane reactor

A pervapoarative membrane reactor is one of the membrane reactors for yield-enhancement of equilibrium-limited reactions. The concept was firstly proposed by Jenning and Binnings in 1960. While a reaction takes place in liquid phase, a by-product (usually water) is removed through a polymeric membrane in the permeate stream. The downstream pressure is kept below the vapor pressure of permeating species. The downstream side is evacuated by a vacuum pump or at least using an inert sweep gas as illustrated in Figure 2.4a and 2.4b respectively.

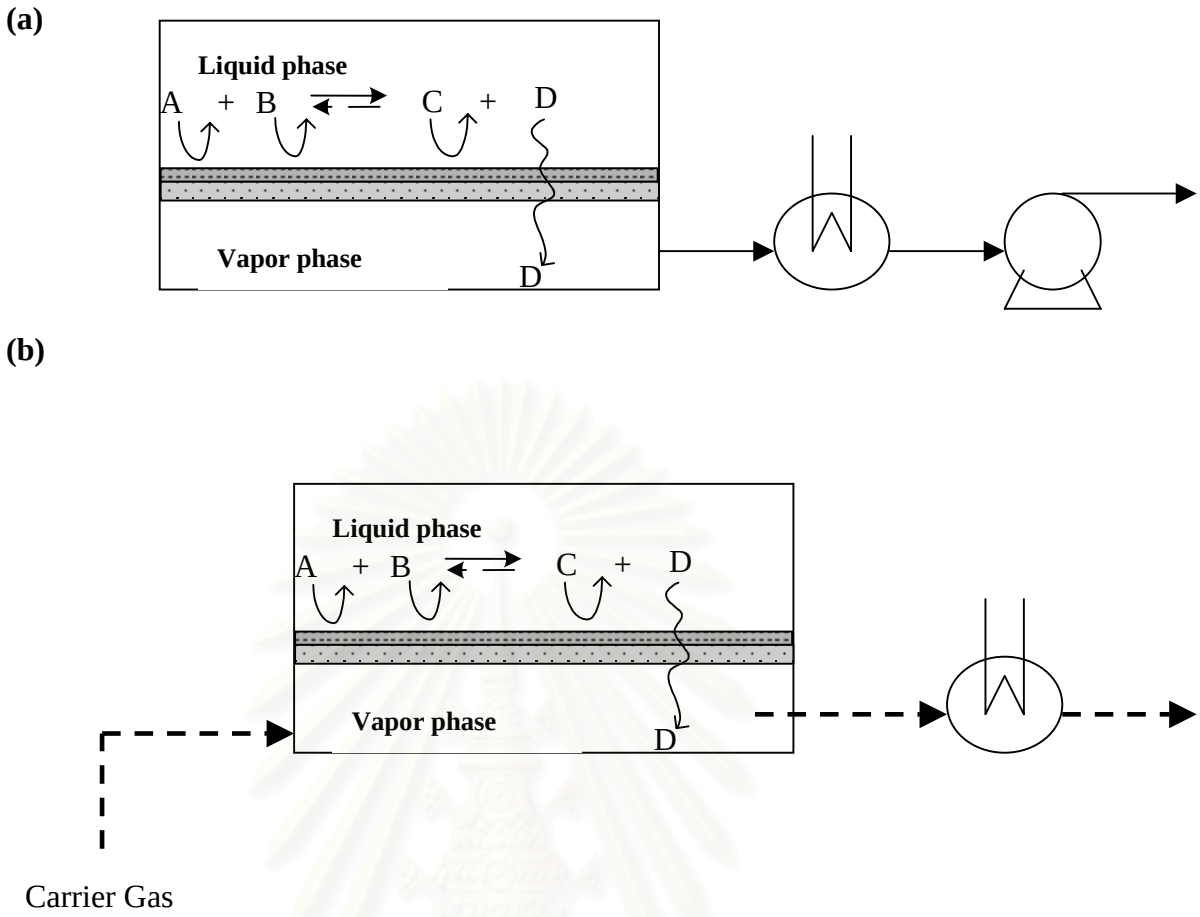

Figure 2.4 Schematic of a typical pervaporative membrane reactor:

(a) using vacuum pump

(b) using inert carrier gas.

2.5 β-Zeolite catalyst

β-Zeolite is an old zeolite discovered before Mobil began the "ZSM" naming sequence. As the name implies, it was the second in an earlier sequence. β-Zeolite was initially synthesized by Wadlinger *et al*. (1995) using tetraethylammonium hydroxide as an organic template. The structure of β-zeolite was only recently determined because the structure is very complex and interest was not high until the material became important for some dewaxing operations. From studies of Treacy and Newsam (1988), and Higgins *et al*. (1986), β-zeolite is an intergrowth hybrid of two distinct but closely related structures that have tetragonal and monoclinic symmetry.

In both systems, straight 12-membered ring channels are present in two crystallgraphic directions perpendicular to [001], while the 12-membered ring in the third direction, parallel to the c axis, is sinusoidal. The sinusoidal channels have circular openings (5.5 Å), and the straight channels have elliptical openings. The only difference between the two polymorphs is in the pore dimension of the straight channels. In tetragonal system, the straight channels have elliptical openings. In tetragonal system, the channels have openings of 6.0x7.3 Å, whereas in the monoclinic system they are 6.8x7.3 Å.

This zeolite may offer interesting opportunities as a catalyst, since it combines three important characteristics: large pores (12-membered oxygen ring), high silica-to-alumina synthesis ratio and tridirectional network of pores. In addition, the dimensions of one type of pores (5.5 Å) can give a certain level of size and shape selectivity. This has been shown to apply to isomerization of C_4-C_7 hydrocarbons to gasoline fractions with increasing octane value, to transalkylation of xylenes, and to condensation of benzene and formaldehyde (Panichsarn *et al*., 1999).

2.6 Catalyst support for the pervaporative membrane reactor

At the Delft University of technology, technology has been developed to prepare binderless films of catalytically active zeolite crystals on metal and ceramic supports. In short, the preparation procedure consists of immersing the support structure in an aqueous solution containing the reactants for zeolite synthesis, after which the system is heated and zeolite crystals grow on the surface of the support (Oudshoorn *et al*., 1999).

However, the commercial ceramic supports, ceramic monoliths, have large pores and low surface areas, so it is necessary to deposit a high surface area carrier, which is subsequently catalyzed, onto the channel wall. The catalyzed coating is composed of a high surface area materials such as Al_2O_3 which will be subsequently impregnated with a catalytic component such as Pt. This referred to as the catalyzed washcoat, illustrated in Figure 2.5. The washcoat depends primarily on the geometry of the channel and the coating method. The pollutant-containing gases enter the

channels uniform and diffuse to the catalytic sites where they are converted catalytically to harmless products.

Monoliths offer a number of design advantages that have led to their widespread use in environmental applications such as catalytic converter used for automotive emissions control. However, the most important advantage is the low pressure drop with high flow rates. The monolith which has a large open frontal area and with straight parallel channel offers less resistance to flow than that of pellet-type catalyst.

Monoliths are generally fabricated from ceramic or metal. The characteristics and properties of both types of monolith are described below.

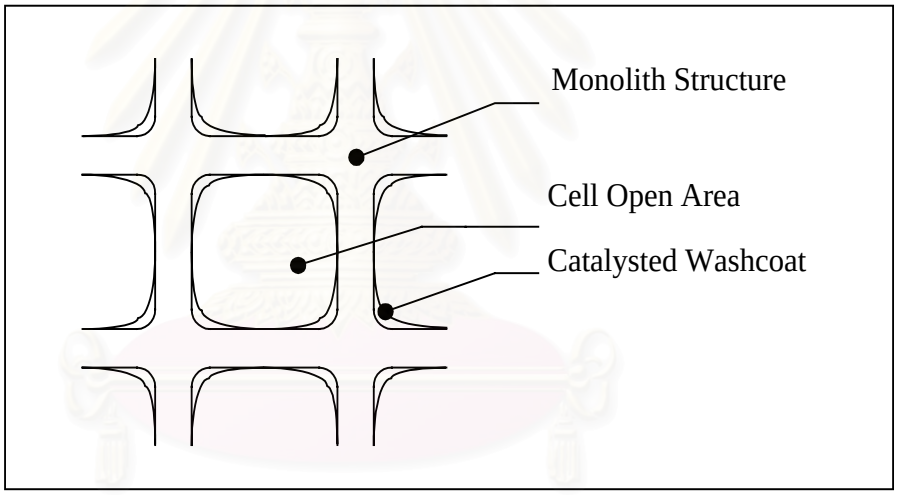

Figure 2.5 Ceramic monolith coated with a catalyzed washcoat.

Ceramic monolithic supports are made of alumina and related materials such as cordierite ($Al_4Mg_2Si_5O_{18}$), mullite ($3Al_2O_3SiO_2)_2$, spoumene ($LiAl(SiO_3)_2$), and asbestos ($Mg_3(Si_2O5)_2(OH)$).

Synthetic cordierite, the first mentioned above, is by far the most commonly used ceramic for monolithic catalyst support applications. Raw materials such as kaolin, talc, aluminium hydroxide, and silica are blended into a paste and extruded

and calcined. It is possible to produce sizes up to about 27.94 cm in diameter and 17.78 cm long, with cell densities from 9 to 600 cells per square inch (cpsi). The conversion desired, the physical space available for the reactor, and engineering constraint such as pressure drop are considered when designing the monolith size.

Cordierite monolith posses several important properties that make these materials preferable for use as a support. These properties are described below.

Thermal shock resistance

By nature of its low thermal expansion coefficient ($10x10^{-7}$/K), cordierite undergoes little dimensional change when cycled over a wide temperature range. Thus, it resists cracking due to thermal shock.

The washcoat influences the thermal shock resistance of the monolith (especially during rapid temperature changes) because it expands more than the monolith. Particle size of the carrier and thickness of the washcoat are two key parameters that must be optimized.

Mechanical strength

Monoliths are made with axial strengths of approximately over 210 kilograms per square centimeter. They must be resistant to both axial and mechanical perturbations experience in automotive, truck, and aircraft applications. The high mechanical integrity is derived from the physical and chemical properties of the raw materials and the final processing after extrusion.

Melting point

The melting point of cordierite is over 1,573 K far greater than temperature expected for modern environmental applications. The materials are also resistant to harsh environmental such as high temperature, stream, sulfur oxides, oil additive constituents, that are present in many exhaust sources.

Catalyst compatibility

Automotive ceramic monolith have well designed pore structure (approximate 3-4 micron) that allow good chemical and mechanical bonding to the washcoat. The chemical component in the ceramic are strongly immobilized, so little migration from the monolith into the catalyzed washcoat occurs.

CHAPTER III
LITERATURE REVIEWS

The synthesis of ETBE is a typical example of equilibrium-limited reaction and the conversion is generally low due to limits imposed by thermodynamic equilibrium. Thus, a combined process of separation and chemical reaction in a single unit operation such as a membrane reactor has attracted much attention for overcoming the equilibrium conversion. In this chapter, the literature reviews on two topics of ETBE synthesis and pervaporative membrane reactor are provided as follows.

3.1 ETBE synthesis

Generally, ETBE can be produced by an exothermic reversible reaction between EtOH and isobutene (IB). However, the supply of IB which is mainly obtained from refinery catalytic cracking and steam cracking fractions becomes limited due to the increased demand of MTBE and ETBE. Hence, alternative routes for the synthesis of ETBE are currently explored (Rihko *et al*.,1996). *Tert*-butyl alcohol (TBA) which is a major by product of propylene oxide production from isobutene and propylene in the ARCO process, can be employed instead of IB as a reactant in this study (Yang and Goto, 1997). TBA was firstly used for the ETBE synthesis over 60 years ago (Norris and Rigby, 1932).

There are two routes to produce ETBE from TBA; namely direct and indirect methods. In the indirect methods, TBA is dehydrated to IB in a first reactor and then the produced IB reacts with EtOH to produce ETBE in a second reactor. In the direct method, ETBE can be produced directly from TBA and EtOH in one reactor. This process is favorable not only because it shortens the process itself, but also because it would reduce demand to the purity of EtOH. Since the reaction itself produces water, the content of water in EtOH becomes insignificant (Yin *et al*.,1995).

There are a number of researches investigating the ETBE synthesis by the direct method on both catalyst screening and kinetic parameter determination.

Several acid catalysts have been employed, for examples Amberlyst-15, heteropoly acid and potassium hydrogen sulfate. The use of a solid ion-exchange resin as catalysts has some advantages over a homogeneous catalyst, for example the catalyst can be easily separated from a solution, and continuous operations are possible. Potassium hydrogen sulfate showed superior performance to Amberlyst-15 (Matouq *et al*., 1996). Heteropoly acid ($H_{0.5}Cs_{3.5}SiW_{12}O_{40}$) yielded superior activity compared to Amberlyst-15, The selectivities of heteropoly acid and Amberlyst-15 at 338 K were 79% and 43% respectively. However, heteropoly acid was significantly inhibited by the presence of water (Yin *et al*., 1995). Comparison between a fluorocarbon sulfonic acid resin catalyst and Amberlyst-15 showed that both catalysts provided almost the same activity; however, the fluorocarbon sulfonic acid catalyst was more thermally stable. ZSM-5 catalyst provided relatively low activity compared to other catalysts (Cunill *et al*., 1993). Recent research compared three cation-exchange resins of S-54, D-72 and Amberlyst-15. It was observed at T = 338 K that S-54 showed the improvements of activity and selectivity of 6 and 5%, respectively, compared to those of Amberlyst-15 while the improvements were 10 and 1% respectively for D-72. (Yang *et al*., 2000).

Zeolitic catalyst showed promising properties on high thermal stability and no acid fume emission against conventional resin-based catalysts (Oudshoorn *et al*., 1999). β-Zeolite may offer interesting opportunities as a catalyst, since it combines three important characteristics: large pores (12-membered oxygen ring), high silicon-to-alumina synthesis ratio and tridirectional network of pores. In addition, the dimensions of one type of pore (5.5 Å) can give a certain level of size and shape selectivity. However, since diameter of β-zeolite powder is very small, the concentration polarization may take place in a pervaporative membrane reactor. To reduce this effect, binderless films of catalytically active zeolite crystals on ceramic supports was developed (Tungudomwongsa *et al*.,1997)

3.2 Pervaporative membrane reactor

The major investigations on the membrane reactors have been concentrated on the inorganic membrane reactors because of their excellent thermal stability at high reaction temperatures. The inorganic membrane reactors have been mainly applied to the reactions concerned with small molecules such as catalytic dehydrogenation, hydrogenation, and decomposition reactions. Polymer membrane reactors, on the other hand, have versatile applicability because the separation capability of polymer membrane depends not only on diffusivity but also on solubility. The polymer membrane reactors can be directly applied to the low temperature chemical reactions with versatile applicability. The majority of published work on polymeric membrane reactor to date is in the field of biotechnology. The membranes used are typically microporous, and the function of the membranes is mainly for immobilizing enzymes, eliminating product inhibition, recycling enzymes and other catalysts, and manipulating substrates and nutrients. For liquid-phase reversible reactor, ultrafiltration membranes are too porous to affect efficient separation of small liquid molecules, while reverse osmosis membranes are likely to require an inconveniently high operating pressure due to osmotic pressure of the reaction mixtures.

Pervaporation, an emerging membrane process specially used for organic-water and organic-organic separations (Huang, 1991), seems to be an appropriate choice. In this process the mass transport through the membrane is induced by maintaining a low vapor pressure on the downstream side, thereby eliminating the effect of osmotic pressure.

The concept of using pervaporation to remove by-product species from reaction mixtures was proposed during the early state of pervaporation research (Jennings and Binnings, 1960). The application of pervaporative membrane reactor is mainly focused on the first application: yield enhancement. However, relatively little literature reports regarding studies on pervaporation membrane for liquid-phase reversible reactions due to lack of suitable membranes with good permselectivity and solvent resistance. During the last decades a number of water permeable membranes with good permeation flux, chemical and thermal stability have been developed, so the interest in pervaporation membrane reactor was rekindled recently when

pervaporation has proven to be a viable separation technique in the chemical industry. Presently, the pervaporation is best applied to dehydration of organic solvents, and the dehydration membranes normally work best when water content in feed mixture is not high. Thus, the pervaporation suitable for reversible reactions that produce by-product water in the reaction enhancement.

Esterification of carboxylic acids and alcohols and etherification with two kinds of alcohol are typical examples of equilibrium-limited reactions that produce by-product water. The conversion is generally low due to limits imposed by thermodynamic equilibrium. To achieve a high yield, it is customary to drive the position of the equilibrium to the ester or ether side by either using a large excess of one of reactants or using reactive distillation to accomplish in situ removal of product (s) (Reid, 1952). The use of a large excess of reactant is accompanied with increased cost for subsequent separation operations, while reactive distillation effective when the difference between the volatility of product and the volatility of reactant species is sufficiently large. In the cases where the reaction mixtures form an azeotrope, a simple reactive distillation configuration is inadequate and also if use large reflux ratio, energy consumption can be significant. Moreover, in reactive distillation the preferred temperature range of reaction should match that for the distillation. In the case of the production of temperature-sensitive product or using biocatalytic conversion, the application of distillation can be impossible due to temperature constraints. In practice, the process performance and energy consumption in reactive distillation are often dominated by distillation operations, as is the case for manufacture of ethyl acetate and other esters (Reid, 1952).

To avoid the above mentioned problems, membrane separation can be considered as a viable alternative due to the following considerations:

1. Pervaporation is a rate-controlled separation process, and the separation efficiency is not limited by relative volatility as in distillation.
2. In pervaporation only a fraction of feed that is permeated by membrane undergoes the liquid phase to vapor phase change, and thus energy consumption is generally low as compares to distillation.
3. With an appropriate membrane, pervaporation can be operated at temperature that matches the optimal temperature for reaction.

4. Since no extractant is used, further purification of the extracted solute, i.e., the permeate, is not necessary provided that the component preferentially permeated is selective enough.
5. The membrane does not need to be regenerated as in the adsorption process.
6. In an industrial scale, it is more flexible to scale up or scale down.

3.2.1 Pervaporative membrane reactor for etherification

There are a number of works on developing new processes to improve the etherification yield. Reactive distillation has been used to produce tertiary ethers on a large scale production. However, from the above drawbacks of reactive distillation, the pervaporation unit was combined externally with reactive distillation.

Matouq and coworkers (1994) proposed a process layout combining an external pervaporation process using hydrophilic polyvinyl alcohol (PVA) membranes with reactive distillation for the production of MTBE. Two types of catalysts i.e. ion exchange resin Amberlyst 15 and heteropoly acid for the reaction of methanol and TBA to form MTBE were investigated. HPA showed higher selectivity than the ion exchange resin. It was found that the hybrid process using pervaporation might be effective in removing water.

Yang and Goto (1997) implemented the similar process for the production of ETBE from EtOH and TBA using Amberlyst15 as a catalyst. Microporous hydrophilic hollow fibre membranes were employed in the pervaporation unit to dehydrate in the bottom product of the reactive distillation column. Shifting the reaction equilibrium led to almost doubling of the mole fraction of ETBE product in the top product.

Luo and coworkers (1997) suggested a different approach. They proposed two alternative process layouts for the processing of the top product from the distillation column located after the reactor. In the first layout, the reactor effluent containing 10wt% EtOH was fed to a distillation column and the top product was processed with the pervaporation unit equipped with 30wt% cellulose acetate butyrate (CAB) and 70wt% cellulose acetate propionate (CAP) membranes. The permeate containing

99.34wt% EtOH was recycled to the reactor. The retentate was recycled to the feed position of the distillation column. In the second layout, the effluent from the reactor with 30wt% EtOH was mixed with the top product and then processed in the pervaporation unit. The EtOH-rich permeate of the pervaporation unit was recycled to the reactor, and the retentate was injected into the feed position of the distillation column. Based on the first layout, it was found that the EtOH recovery of 99.34wt% using the hybrid process was significantly higher compared with the conventional process of 55.2wt%.

3.2.2 Pervaporative membrane reactor for esterification

The use of pervaporative membrane reactor for esterification is different from the previous combined process of reactive distillation and pervaporation in which H_2O was externally removed from the top or bottom stream. In the pervaporative membrane reactor, the product H_2O was simultaneously removed from the reaction zone while the reaction took place. A number of reactions have been tested in this reactor.

Pervaporative membrane reactor for esterification of oleic acid and ethanol to produce ethyl oleate was studied using p-toluenesulfonic acid as a catalyst (Kita *et al*., 1987-88; Okamoto *et al*., 1993). Polyimide, chitosan, nafion, polyetherimide and perfluorated ion-exchange were used as membranes. Among these membranes, polyimide showed the highest selectivity. Complete conversion could be achieved at about 6 hours when ethanol was in excess.

For ethyl acetate synthesis from acetic acid and ethanol, the first system was operated batchwise using p-toluenesulfonic acid and a polyetherimide membrane (Kita *et al*., 1988). Later the operation was continuous utilizing a polymeric/ceramic membrane. A ceramic support tube was dipped in a polyetherimide solution. Sulfuric acid (96%) was added to an acetic acid syringe and used as the homogeneous catalyst (Zhu *et al*., 1996). Waldburger and coworkers (1994) studied a heterogeneous catalyst in the continuous tube membrane reactor. In the tube membrane reactor, a hydrophillic polyvinyl alcohol (PVA) membrane was placed on a sintered tube as a support. The equimolar feed of mixture was fed and an ethyl acetate yield of 92.1%

was obtained with a water concentration of 0.5wt% in the product stream. Using a cascade of three membrane reactors the ethyl acetate yield was increased to 98.7% and the water concentration was reduced to 0.1wt%. An economic assessment was studied. It was found that, compared to the conventional process, the pervaporation-based membrane reactor could cut energy costs by over 75% and operating costs by 50%.

David and coworkers (1991) studied the esterification of 1-propanol and 2-proponol with propionic acid to produce propyl propionate and iso-propyl propionate. Pervaporation with PVA membranes was externally added to the reactor. It was revealed that the hybrid process was governed by four main parameters that influenced the conversion rate: in order of significance, these are temperature, initial molar ratio, membrane area to reaction volume ratio, and catalyst concentration.

Most of the models presented so far of pervaporative membrane reactor describe both the kinetics and membrane permeation in term of concentrations of the reacting species.

For thermodynamically nonideal mixtures, however, activites are needed in the description of transport (pervaporation) by a solution diffusion mechanism through the membrane. For nonideal reacting mixtures, furthermore, expressing the reaction rates in terms of concentration results in reaction rates constants which often depend on concentrations since the latter do not completely take into account the interactions between molecules. The use of activities not only rectifies this problem but also provides a unified approach in treating both the thermodynamic equilibrium and the driving force in the rate equation. Several authors have made use of activities for the description of esterification reaction rates.

A continuous pervaporation membrane reactor for the esterification of acetic acid and ethanol to produce ethyl acetate was studied by Zhu *et al*.(1996). Hydrophilic polymeric/ceramic composite membrane were used for pervaporation. Comparing the reactor conversion rates under different experimental conditions it was discovered that the rates were higher than expected from the reaction equilibrium

data. A theoretical activity-based model was developed which showed a reasonable fit of the experimental results.

Krupicka and Koszorz (1999) studied in the same reaction. A comparison of the measured concentrations with those calculated according to the model showed sound agreement when the activities were used. The experiments were performed using a wide range of initial molar ratios with commercial hydrophilic PERVAP 1105 GFT membrane. The model was independent of the initial molar ratios due to the stability of thermodynamic and kinetic constants.

Due to simplicity of a concentration-based model, some researches still explained the models in term of concentrations. In a parameter study, Feng and Huang (1996) revealed that reaction and conversion rate could be improved. It was discovered that a complete conversion could be achieved if one reactant was in excess. Membrane area and permeability as well as the volume of the mixture to be treated were identified as the important parameters of the process. Furthermore, it was shown that the operating temperature influenced both the reaction and membrane permeation rate. Lucilia and coworkers (1996) studied a pervaporative membrane reactor for the esterification of acetic acid and benzyl alcohol by applying p-toluenesulfonic acid as a catalyst to form benzylacetate. In both cases concentration-based models were used to determine the kinetic parameters. A theoretical model was developed and satisfactorily agreed with the obtained experimental results.

Several simulations were performed with the use of presented model to indicate the influence of the ratio of membrane area (*A*) to volume (*V*) or mass (*M*) of mixtures on the concentrations in reaction mixture. The efficiency of the process was strongly related to *A/V* or *A/M* ratio. Increasing the value of *A/V* or *A/M*, can efficiently shift the reaction equilibrium and obtain a reasonably pure ester directly after the reaction. Selection of the *A* and *V* values to be used was determined from an economic point of view.

The application of a pervaporative membrane reactor for the esterification of tartaric acid and ethanol to form diethyltartarate was studied by Keurentjes *et al.* (1994). The equilibrium composition could be significantly shifted towards the final

product diethyltartarate by intregrating pervaporation, equipped with PVA composite membranes, into the process. The kinetic parameters were established. Both concentration-based and activity-based reaction rate constants and equilibrium constants were determined. The activity-based data were determined using UNIFAC activity coefficient estimations. It can be concluded that reaction rate constants determined in dilute solutions are capable of describing the reaction in a concentrated environment. This applies both for the activity-based description as well as for the concentration-based description. Although the activity coefficients involved differ significantly from unity, the effects of the individual activity coefficients are mutually compensated. Therefore, it is also possible to predict the reaction correctly when the concentration-based parameters are used.

CHAPTER IV

EXPERIMENTAL

This chapter describes the experimental procedures for the synthesis of ethyl *tert*-butyl ether (ETBE) from ethanol (EtOH) and *tert*-butyl alcohol (TBA) in both semi-batch reactor and pervaporative membrane reactor. Details are given for the catalyst and supporting material preparation, kinetic study, permeation study and pervaporative membrane reactor study as follows.

4.1 Catalyst and supporting material preparation

4.1.1 Preparation of β-zeolite powder

The reagents used for the synthesis of β-zeolite is shown in Table 4.1. The preparation processes consists of the following steps.

Table 4.1 Reagents used for the preparation of β-zeolite.

Items	Weight x 10^{-3} (kg)
TEAOH	6.2
Cataloid for Si/Al = 50	6.7
KCl	0.5
NaOH	0.5
NaAlO2	0.7
NaCl	0.4

4.1.1.1 Gel preparation

Tetraethylammonium hydroxide (40% by weight aqueous solution) was mixed with sodium hydroxide and stirred until it became a homogeneous solution. The mixed solution was added with sodium aluminate (Al/NaOH about 0.81), potassium chloride and sodium chloride. Then it was stirred to obtain a clear solution at the room

temperature. Cataloid (SiO_2 30% by weight aqueous solution) was added dropwisely to the mixed solution. A vigorous stirrer was applied for one hour to obtain a gel.

4.1.1.2 Crystallization

The obtained gel was stirred thoroughly before transferring it to a stainless-steel autoclave. The gel was heated in the autoclave from the room temperature to 408 K in 60 min. under the nitrogen pressure of 3 kg/cm^2 (gauge) and maintained at this temperature for 40 hours. Then, the autoclave was immersed in cold water to start a crystallization process. The obtained solid material was centrifuged at 2,500 rpm (about 15 min) and the recovered solid were washed and dried in an oven at 383 K overnight.

4.1.1.3 First calcination

The dry solid was calcined in an air stream at 813 K for 3.5 hours by heating it from the room temperature to 813 K in 1 hour. This step was to burn off the organic template and leave the cavities and channels in the crystals. Then, the calcined crystals were cooled to the room temperature in a desiccator. After this step, the crystals formed were called Na β-zeolite.

4.1.1.4 Ammonium ion-exchange

The ion-exchange step was carried out by mixing the calcined crystal with 2 M NH_4NO_3 (ratio of catalyst and solution is 1g:30 cm^3) and heated on a stirring hot plate at 353 K for 1 hour. The mixture was cooled down to the room temperature. Then, the ion-exchange crystal was washed twice with de-ionized water and then separated by using centrifugal separator. After that, the ion-exchange crystal was dried at 383 K for at least 180 min. in the oven. The dried crystals (NH_4β-zeolite) were obtained.

4.1.1.5 Second calcination

The removable species, i.e. NH_3 and NO_X were decomposed by thermal treatment of the ion-exchange crystals in a furnace by heating them from the room temperature to 773 K in 1 hour in air stream and maintained at this temperature for 2 hours. After this step, the obtained crystals were H-β-zeolite which was used for kinetic study.

4.1.2 Preparation of supported β-zeolite

Supported β-zeolite was used in kinetic and pervaporative membrane reactor studies. The catalyst was made by coating the obtained powder catalyst on a cordierite monolith obtained from N-COR Ltd., Nagoya, JAPAN. The procedures are as follows:

4.1.2.1 Preparation of monolith sample

The monolith test samples were prepared by cutting the cordierite monolith (400 cell/in^2) into small cube support (0.5x0.5x0.5 cm^3).

4.1.2.2 Surface treatment

The monolith supports were weighed and soaked in 2.5 wt% acetic acid solution for 2 min. After that, they were washed by distilled water several times to remove residual acid solution and then dried in an oven at 383 K until the weight became constant.

4.1.2.3 Preparation of slurry for washcoat

β-Zeolite powder was added into 2.5 wt% acetic acid solution to give 30-50 % wt/volume β-zeolite washcoat and the obtained slurry was stirred for 5-10 min.

4.1.2.4 Monolith coating procedure

The monolith supports were dipped into the prepared washcoat for 15 min. and followed by drying at 383 K overnight in the oven. The supports were repeatedly dipped in the washcoat 2-3 times and calcined at 773 K for 3.5 hours in air atmosphere.

4.1.3 Characterization of the catalysts

4.1.3.1 X-ray diffraction patterns

X-ray diffraction (XRD) patterns of the catalysts were performed with SIEMENS XRD D5000, accurately measured in the 4-44° 2θ angular region, at petrochemical Engineering Laboratory, Chulalongkorn University.

4.1.3.2 X-ray fluorescence spectrometer

The composition of β-zeolite was examined by using an X-ray fluorescence spectrometer (XRF-model Fision)

4.2 Kinetic study

4.2.1 Batch reactor apparatus

Kinetic study of the supported β-zeolite was carried out in a specially-designed reactor as shown in Figure 4.1. A jacket reactor was maintained at a constant temperature by circulating hot water in jacket around the chambers. A heater with a temperature controller was used to control a water temperature while a condenser was equipped with the system to condense all vapors in the reaction chamber. The reactor had four connectors for connecting a condenser, a rotating shaft, sampling port and thermocouple. A frame of four catalyst baskets (as illustrated in Figure 4.2) was equipped with a rotating shaft which was driven by a motor via an inverter controller.

The cylindrical baskets were made of stainless steel tubes with a wall made of stainless steel mesh.

4.2.2 Experimental procedure

1. The catalyst was left in an oven at 363 K overnight to remove moisture from the catalyst and a certain amount of catalyst was weighted.
2. 2 moles of EtOH and TBA were placed into the reactor.
3. The supported catalyst with 15 g of β-zeolite powder / or 15 g of Amberlyst 15 catalyst was packed in four catalyst baskets.
4. The frame was held above the liquid level by upper hooks as shown in Figure 4.2 (a) to prevent the reaction occurring.
5. Four-bladed disk turbine was used to stir the liquid mixture during heating up period.
6. After temperature was maintained at a desired value, the reaction was started by inverting the direction of agitation so that the frame of baskets dropped into the liquid mixture. The lower hooks were securely connected with slots on the disk turbine and the frame was rotated with slip as shown in Figure 2.2(b). The desired temperature and stirring speed were shown in Table 4.2.
7. Liquid samples of 1 cm^3 were taken to measure concentrations of H_2O, EtOH, TBA, IB and ETBE at different reaction times: i.e. 0, 0.5, 1, 1.5, 2, 2.5, 3, 3.5, 4, 5, 6, 7 hours. They were analyzed by a gas chromatography. The operation condition of the gas chromatography was shown in Table 4.3.

Table 4.2 Operating condition for kinetic study

Catalyst weight	15 g
Reaction temperature	323, 333, 343 K
Atmospheric pressure	
Reaction time	0-7 h
Mole of Ethanol	2 mol
Mole of TBA	2 mol
Speed Level of stirrer	880, 1210, 1350 rpm

Table 4.3 Operating condition of gas chromatography

Model	GC 8A
Detector	TCD
Packed column	Gaskuropack 54
Column length	2.5 m
Mesh size of packing	60/80
Helium flow rate	30 cm^3/min
Column temperature	443 K
Injector temperature	453 K
Detector temperature	443 K

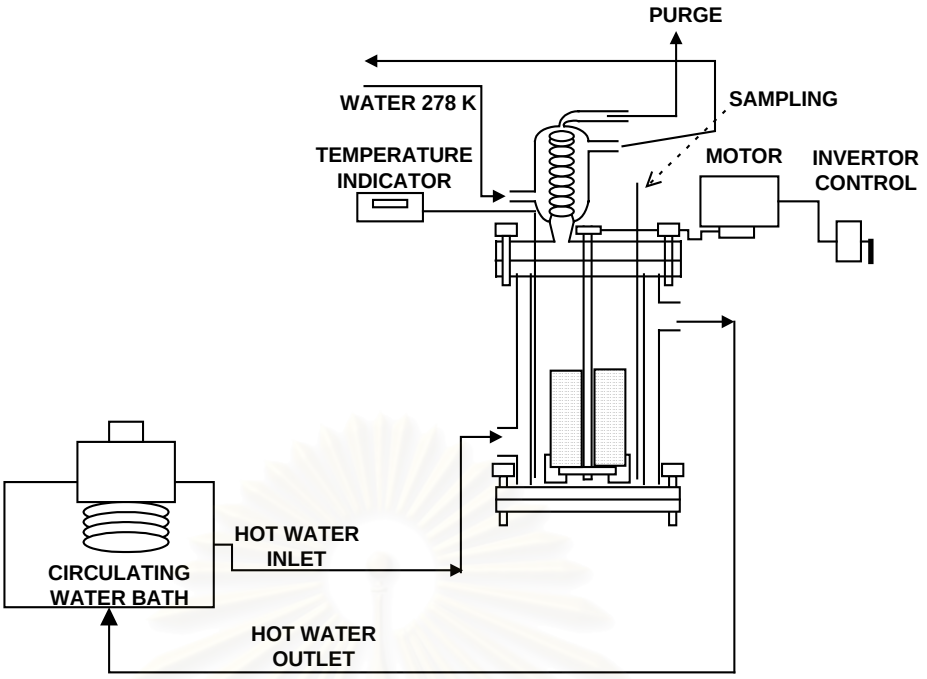

Figure 4.1 Schematic diagram of the kinetic studied experimental set-up

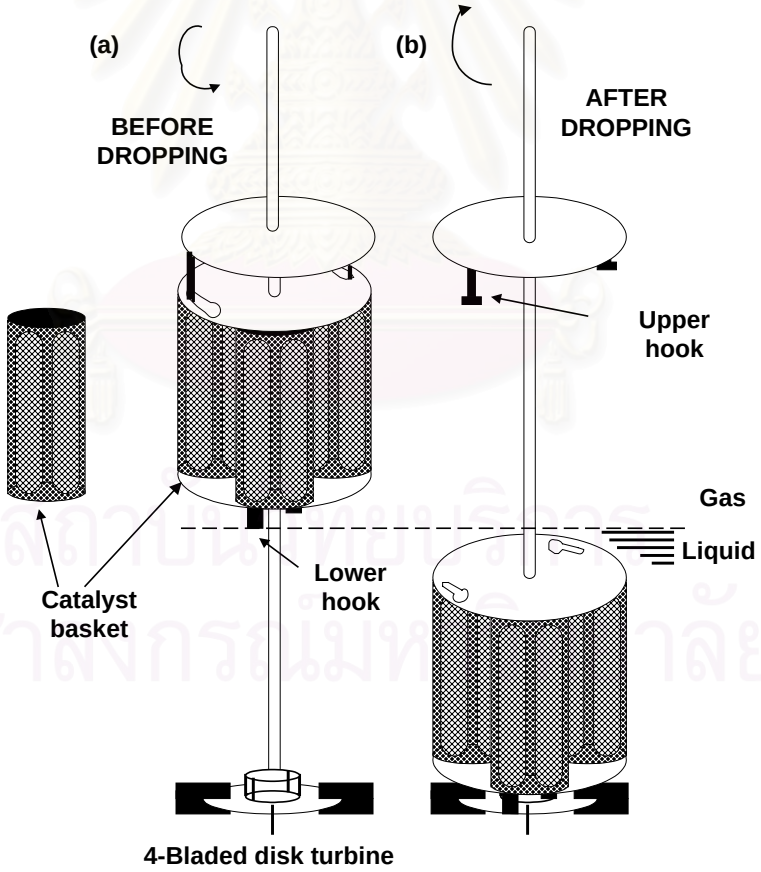

Figure 4.2 Detail of catalyst basket assembly.
(a) Before dropping
(b) After dropping

4.3 Permeation study

4.3.1 Permeation measurement apparatus

Figure 4.3 shows a schematic diagram of the permeation measurement apparatus. The membrane with an effective area of 54 cm^2 was placed between two chambers and sealed with silicone O-ring. A disk turbine was used to stir the liquid mixture in the upper chamber to ensure well-mixed condition. The lower chamber called “permeate side” was fed with a N_2 sweep gas.

4.3.2 Experimental procedure

1. A membrane was dried at 353 K for 3 h before using.
2. Adjust N_2 sweep gas flow rate at $7.2x10^{-5}$ mol/s, hold for 2 h to ensure the flow rate is constant and remove moisture in line and permeate chamber.
3. Add feed mixture in the upper chamber and heat up to desired temperature.
4. After liquid temperature was maintained at a desired value, it assumed start up permeate at this time.
5. Permeation rate of each species was obtained by measuring a permeate flow rate by a bubble flow meter and gas samples of 2 cm^3 were taken to measure concentrations of H_2O, EtOH, TBA, IB, ETBE and N_2 at different times: i.e. 0.5, 1, 1.5, 2, 2.5 and 3 hours by the gas chromatography.

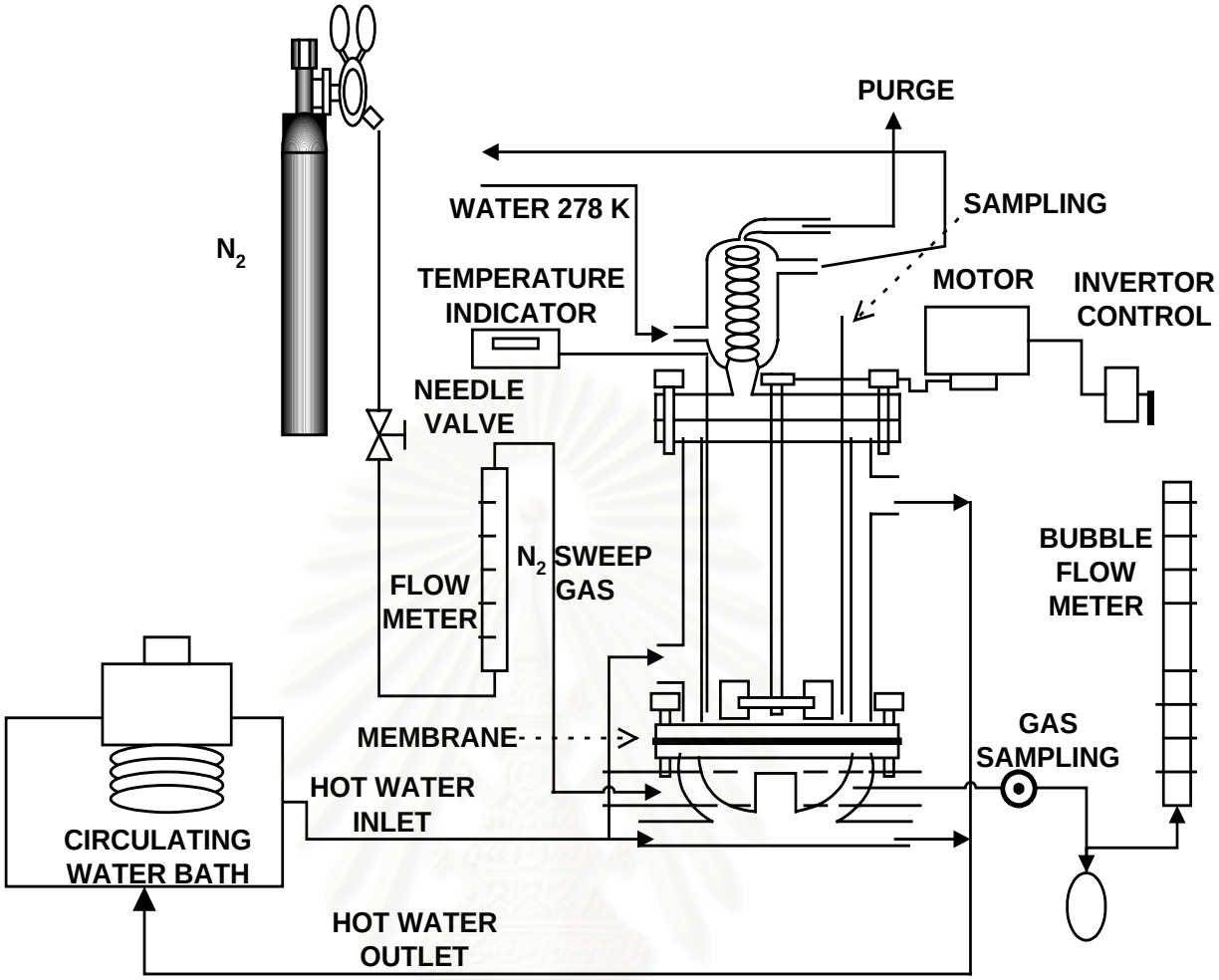

Figure 4.3 Schematic diagram of the permeation studied experimental set-up

4.4 Pervaporative membrane reactor study

The pervaporative membrane reactor was carried out in the same apparatus used for the permeation study in Figure 4.3; however, the catalyst baskets (as illustrated in Figure 4.2) were equipped.

4.4.1 Experimental procedure

1. A membrane was dried at 353 K for 3 hours before use.
2. The catalyst was left in an oven at 363 K overnight to remove moisture from the catalyst and a certain amount of catalyst was weighed.
3. Adjust N_2 sweep gas flow rate at $7.2x10^{-5}$ mol/s, hold for 2 hours to ensure the flow rate was constant and remove moisture in line and permeate chamber.
4. 2 moles of EtOH and TBA were placed into the reactor.
5. The supported catalyst with 15 g of β-zeolite powder was packed in four catalyst baskets.
6. The frame was held above the liquid level by upper hooks as shown in Figure 4.2 (a) to prevent the reaction occurring.
7. Four-bladed disk turbine was used to stir the liquid mixture along heating up.
8. After the operating temperature was maintained at a desired value, the reaction was started by inverting the direction of agitation so that the frame of baskets dropped into the liquid mixture. The lower hooks were securely connected with slots on the disk turbine and the frame was rotated with slip as shown in Figure 2.2(b). The desired temperature and stirring speed were shown in Table 4.2.
9. Liquid samples of 1 cm^3 and permeate gas sample of 2 cm^2 were taken to measure concentrations of H_2O, EtOH, TBA, IB, ETBE and N_2 at different reaction times: i.e. 0, 0.5, 1, 1.5, 2, 2.5, 3, 3.5, 4, 5, 6, 7 hours. The concentrations of them were analyzed by a gas chromatography. Permeation rate of each species was obtained by measuring a permeate flow rate by a bubble flow meter.

CHAPTER V

RESULTS AND DISCUSSION

In this chapter, the results and discussion are divided to four sections: characterization of β-zeolites; catalyst selection and kinetic study; permeation study and pervaporative membrane reactor study. Details are as follows.

5.1 Catalyst Characterization

5.1.1 X-ray Diffraction (XRD)

Synthesized β-zeolite was analyzed by an X-ray diffraction for identifying crystal structure. The X-ray diffraction pattern of H form of β-zeolite is illustrated in Figure 5.1. The pattern was corresponding well with those reported by Ramesh *et al*. (1992) as shown in Figure5.2. This indicated that the synthesized catalysts had the same structure as β-zeolite.

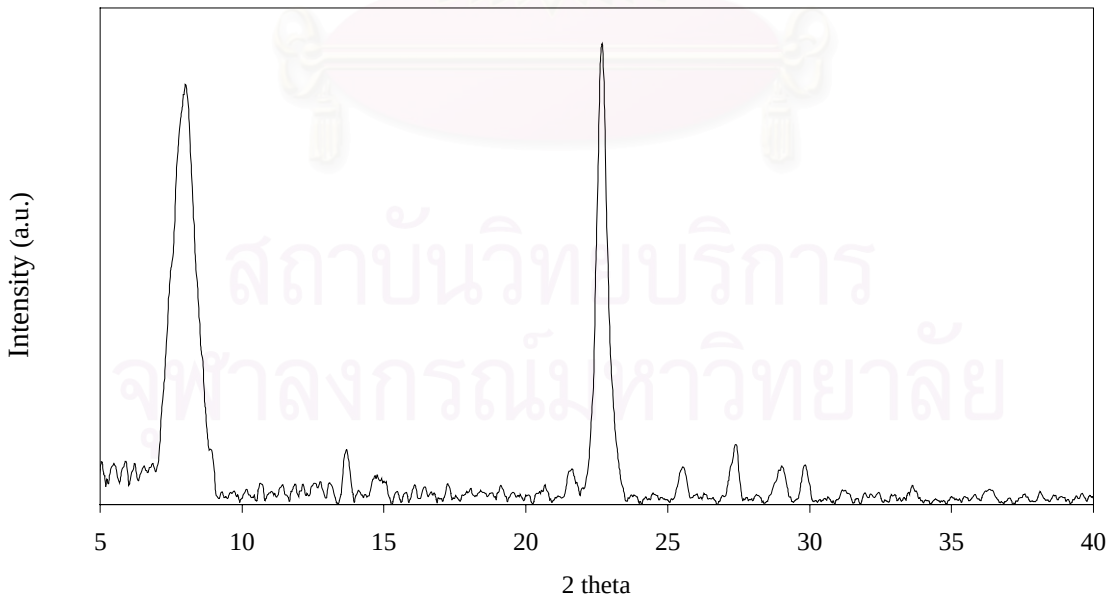

Figure 5.1 X-ray diffraction pattern of β-zeolite.

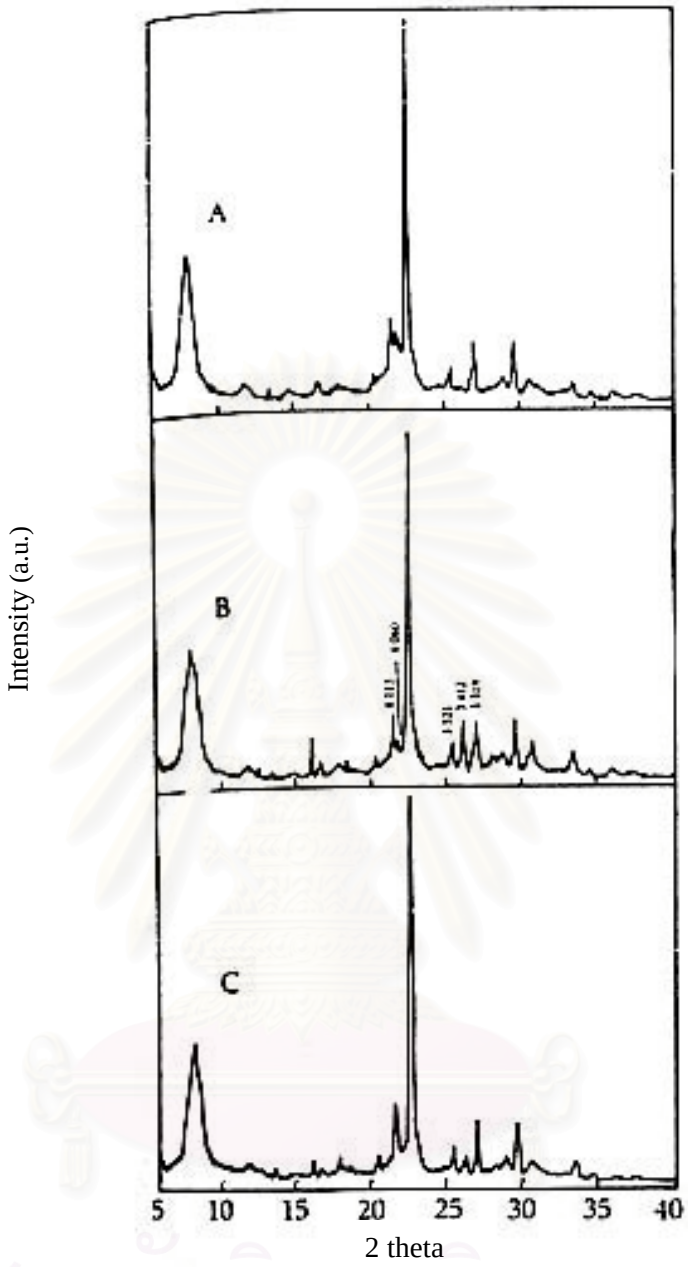

Figure 5.2 X-ray diffraction pattern of β-zeolite (Ramesh *et al*.,1992)
Si/Al : A = 19.7, B = 12.2, C = 10.5

5.1.2 X-ray fluorescence spectrometer (XRF)

Synthesized β-zeolite was analyzed by an XRF to measure the catalyst composition. It was found that the Si, Al and Na contents were 96.97, 2.30 and 0.21 wt%, respectively, thus yielding the Si/Al ratio of 41.

5.2 Comparison between catalysts

Two types of catalysts; i.e. Amberlyst-15 and supported β-zeolite were tested to compare the performance on the synthesis of ETBE from EtOH and TBA. Amberlyst-15 was selected for comparison because it is a commercial catalyst for *tert*-ether synthesis. It is a strong cation exchange resin made of a sulfonated styrene divinyl benzene copolymer with a macroreticular structure. The experiments were carried out at the following condition; i.e. 15 grams of Amberlyst-15 or β-zeolite, T = 333 K, stirring speed = 1210 rpm and the initial amounts of ethanol and TBA were 2 and 2 mol, respectively. The reactions taking place in the reactor can be summarized as follows

$$\text{TBA} + \text{EtOH} \Leftrightarrow \text{ETBE} + \text{H}_2\text{O} \quad (5.1)$$

$$\text{TBA} \Leftrightarrow \text{IB} + \text{H}_2\text{O} \quad (5.2)$$

$$\text{IB} + \text{EtOH} \Leftrightarrow \text{ETBE} \quad (5.3)$$

The yield and selectivity of the reaction system are defined in the following equations.

$$Yield = \frac{m_{ETBE} - m_{ETBE,0}}{m_{TBA,0}} \quad (5.4)$$

$$Selectivity = \frac{m_{ETBE} - m_{ETBE,0}}{m_{TBA,0} - m_{TBA}} \quad (5.5)$$

Figure 5.3 shows the number of moles of TBA, EtOH, ETBE and H_2O at different reaction time of both catalysts. Filled and empty symbols represent results of Amberlyst-15 and β-zeolite, respectively. It should be noted that the side product, IB was mainly present in the gas phase. Considering the disappearance of TBA, it was found that β-zeolite was less active than Amberlyst-15. However, when considering the formation of ETBE, it is obvious that the ETBE yields of both catalysts were almost the same at 12%.

It was investigated that the selectivities of β-zeolite and Amberlyst-15 were 61% and 35% respectively. It can be concluded that β-zeolite was much more

attractive than Amberlyst-15 and, consequently, the following studies would consider only β-zeolite catalyst.

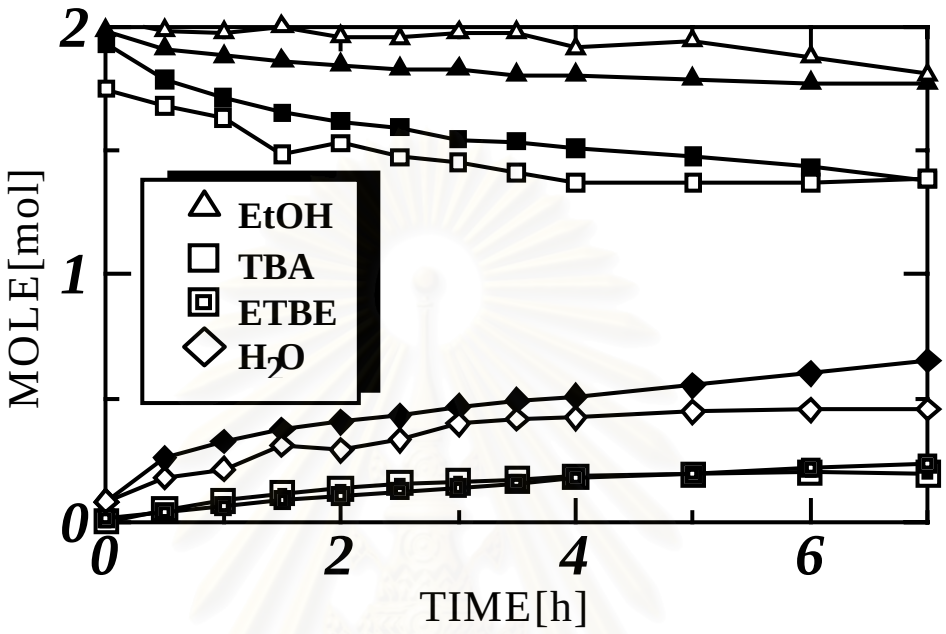

Figure 5.3 Comparison between different catalysts: filled symbols = Amberlyst-15, empty symbols = β-zeolite (Catalyst = Amberlyst-15, catalyst weight = 15.0 g, $m_{TBA,o}$ = 1.93 mol, $m_{EtOH,o}$ = 1.98 mol, $m_{ETBE,o}$ = 0 mol, $m_{H_2O,o}$ = 0.09 mol:
Catalyst = β-zeolite, catalyst weight = 15.0 g, $m_{TBA,o}$ = 1.75 mol, $m_{EtOH,o}$ = 2.04 mol, $m_{ETBE,o}$ = 0.02 mol, $m_{H_2O,o}$ = 0.09 mol and T = 333 K).

5.3 Kinetic study

5.3.1 The effect of external mass transfer

In the kinetic study, the supported β-zeolite was used. The effect of external mass transfer of catalyst was studied by varying stirring speeds. Figure 5.4 shows the relationship between conversion of TBA at 7 h and the stirring speed. It was found that the conversion increased with increasing speed level and, finally, it leveled off at the speed level of 1210 rpm. This can be concluded that the effect of external mass

transfer just constant and cannot be reduced further by increasing stirring speed higher than 1210 rpm. In the subsequent studies, the speed of 1210 rpm was used.

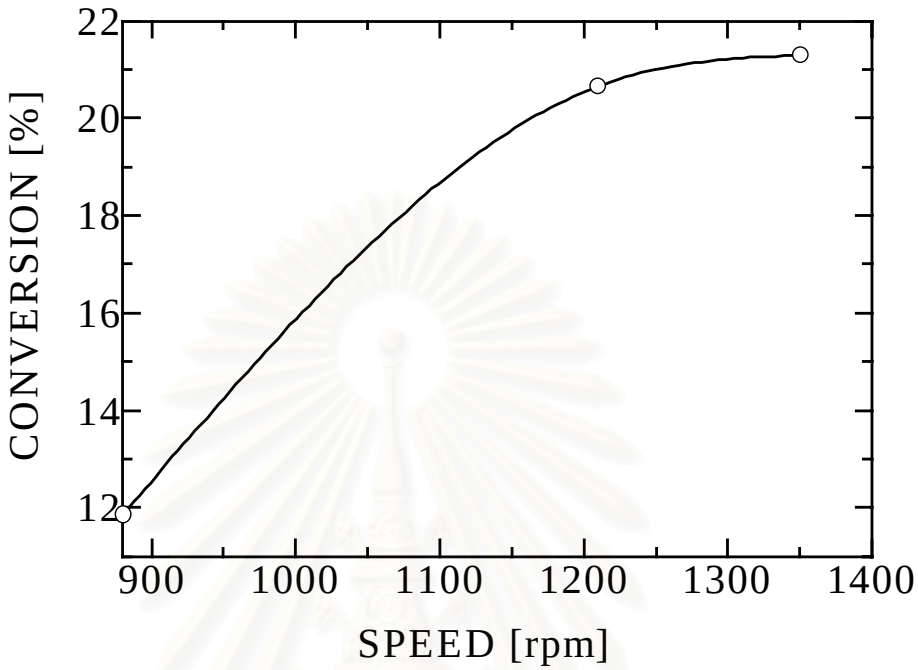

Figure 5.4 The effect of speed level on the conversion (Catalyst = β-zeolite, catalyst weight = 15 g, $m_{TBA,o}$ =2 mol, $m_{EtOH,o}$ = 2 mol, T = 333 K and time = 7 h).

5.3.2 Development of mathematical models

Mathematical descriptions were developed for both concentration-based and activity-based models. The reverse reaction in Eq. (5.2) and the reaction in Eq. (5.3) were neglected since the operating pressure in this study was at atmospheric pressure and, consequently, only small amount of IB can be dissolved in the liquid. It was also confirmed by our experimental results that the concentration of IB in liquid mixture was negligibly small. As a result, the rate laws of the reactions (5.1) and (5.2) can be expressed in terms of concentrations as (Quitain *et al.*,1999)

$$r_1 = k_{1c}\frac{(c_{TBA}c_{EtOH} - c_{ETBE}c_{H_2O}/K_{1c})}{1+K_{Wc}c_{H_2O}} \qquad (5.6)$$

$$r_2 = k_{2c}\frac{c_{TBA}}{1+K_{Wc}c_{H_2O}} \qquad (5.7)$$

and in terms of activities as

$$r_1 = k_{1a} \frac{(a_{TBA} a_{EtOH} - a_{ETBE} a_{H_2O} / K_{1a})}{1 + K_{Wa} a_{H_2O}} \quad (5.8)$$

$$r_2 = k_{2a} \frac{a_{TBA}}{1 + K_{Wa} a_{H_2O}} \quad (5.9)$$

where k_{jc} and k_{ja} are reaction rate constants of reaction j (j = 1, 2) in the concentration-based and activity-based models, respectively. c_i and a_i are concentration and activity of species i, respectively. K_1 is the equilibrium constant. K_{Wc} and K_{Wa} are water inhibition parameters from in the concentration-based and activity-based models, respectively. The expressions of K_{1a} and K_{1c} which are valid within the temperature range of 278-353 K are given as follows (Jensen and Datta, 1995).

$$K_{1a} = \exp(1140.0 - 14580 / T + 232.9 \ln T + 1.087T - 1.114\text{x}10^{-3}T^2 + 5.538\text{x}10^{-7}T^3) \quad (5.10)$$

$$K_{1c} = \exp(10.387 - 4060.59 / T + 2.891 \ln T - 1.915\text{x}10^{-2}T + 5.286\text{x}10^{-5}T^2 - 5.330\text{x}10^{-8}T^3) \quad (5.11)$$

By performing a material balance for a semi-batch reactor, the following expressions are obtained.

$$-\frac{dm_{TBA}}{dt} = \frac{dm_{H_2O}}{dt} = W(r_1 + r_2) \quad (5.12)$$

$$-\frac{dm_{EtOH}}{dt} = \frac{dm_{ETBE}}{dt} = Wr_1 \quad (5.13)$$

where m_i and W represent the number of mole of species i and the catalyst weight, respectively. It is noted that the number of moles in the liquid phase at any time is constant because IB can only slightly dissolved in the liquid phase. In addition, every one mole of TBA consumption produces one mole of water, and every one mole of EtOH consumption produces one mole of ETBE. The activity can be calculated from the following relation.

$$a_i = \gamma_i x_i \quad (5.14)$$

where x_i is mole fraction of species i in the liquid mixture and γ_i is the activity coefficient. The activity coefficients can be calculated using the UNIFAC method (Gmehling *et al*., 1982)

5.3.3 Kinetic parameter determination

A set of experiments was carried out at three temperature levels to investigate the kinetic parameters. Figures 5.5, 5.6 and 5.7 show typical results of mole changes with time at T = 323, 333 and 343 K, respectively. The initial moles of each species were given in the figure captions. It can be seen that the production of ETBE became higher with the increase of temperature as expected in the Arrhenius' equation.

A curve fitting method was employed to find the kinetic parameters, k_{1c}, k_{2c} and K_{wc} for the concentration-based model and k_{1a}, k_{2a} and K_{wa} for the activity-based model at each temperature. Initial guess values of the parameters k_{1c}, k_{2c}, k_{1a} and k_{2a} were obtained by using an initial rate method (Fogler, 1992). The dashed lines in the figures represent the simulation results from the concentration-based model while the solid lines represent those from the activity-based model using the corresponding parameters. It was found that within the ranges of study, both models fit the experimental results well. However, it should be noted that the activity-based model is more suitable for a liquid phase reaction since its performance usually deviates from ideality. Nevertheless, the concentration-based parameters are also included in this study since they can be directly used in simulation on commercial software such as Aspen Plus.

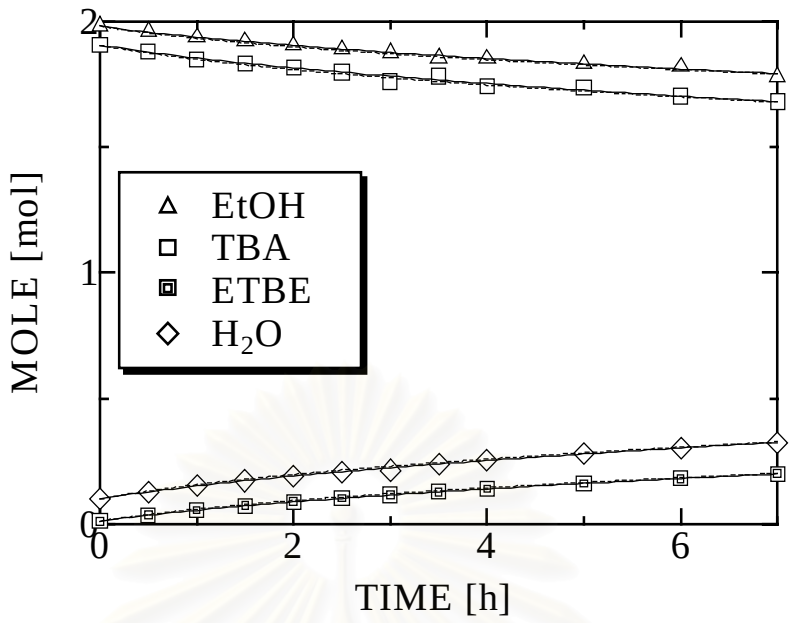

Figure 5.5 Mole changes with time (Catalyst = β-zeolite, catalyst weight = 15.0 g, $m_{TBA,o}$ = 1.91 mol, $m_{EtOH,o}$ = 1.98 mol, $m_{ETBE,o}$ = 0.01 mol, $m_{H_2O,o}$ = 0.10 mol and T = 323 K).

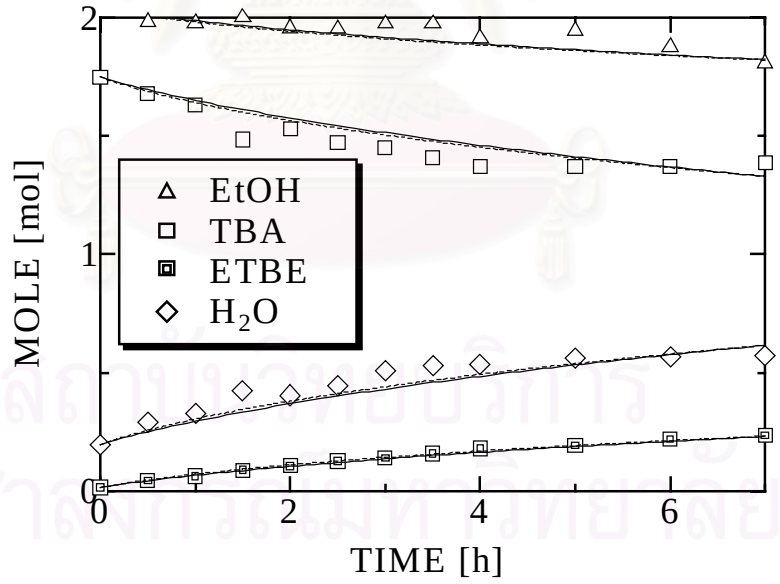

Figure 5.6 Mole changes with time (Catalyst = β-zeolite, catalyst weight = 15.0 g, $m_{TBA,o}$ = 1.75 mol, $m_{EtOH,o}$ = 2.04 mol, $m_{ETBE,o}$ = 0.02 mol, $m_{H_2O,o}$ = 0.20 mol and T = 333 K).

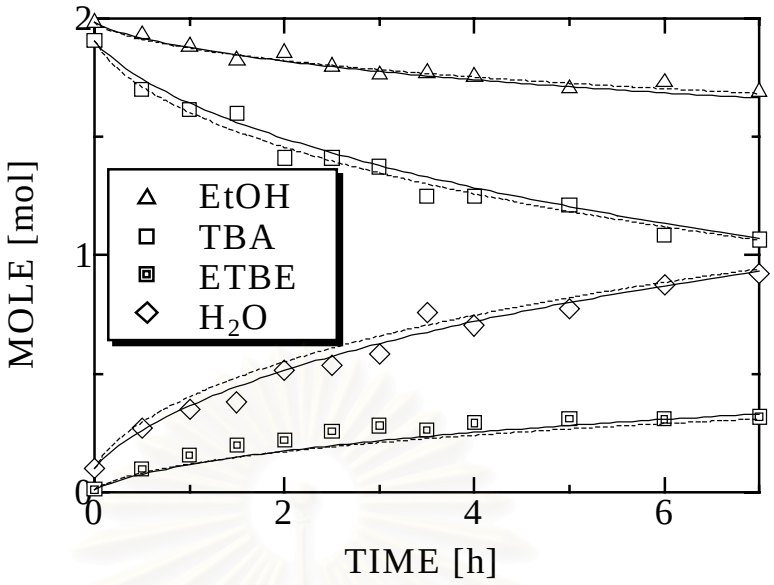

Figure 5.7 Mole changes with time (Catalyst = β-zeolite, catalyst weight = 15.0 g, $m_{TBA,o}$ = 1.91 mol, $m_{EtOH,o}$ = 1.98 mol, $m_{ETBE,o}$ = 0.01 mol, $m_{H_2O,o}$ = 0.10 mol and T = 343 K).

Figure 5.8 shows the Arrhenius plot of the reaction rate constants while Figure 5.9 shows the Van`t Hoff`s plot of the adsorption parameters.

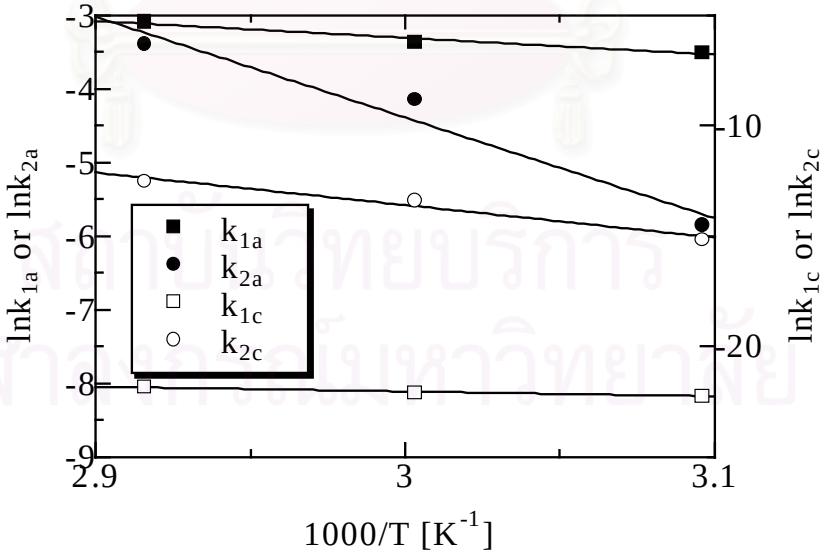

Figure 5.8 Arrhenius plot.

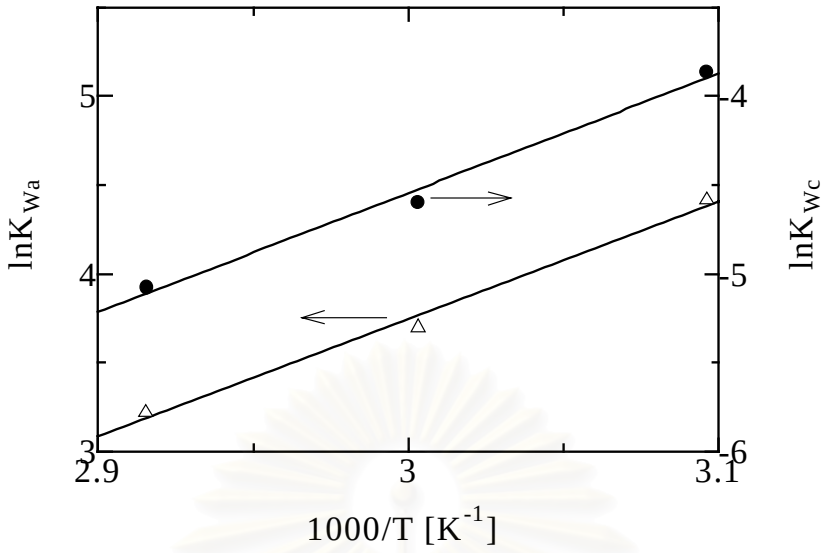

Figure 5.9 Van't Hoff plot.

The following equations were determined from the plots.

Concentration-based model:

$$k_{1c} = \exp(-15.48 - 2186/T) \quad (5.15)$$

$$k_{2c} = \exp(34.47 - 14688/T) \quad (5.16)$$

$$K_{Wc} = \exp(-24.72 + 6725/T) \quad (5.17)$$

Activity-based model:

$$k_{1a} = \exp(3.55 - 2286/T) \quad (5.18)$$

$$k_{2a} = \exp(36.57 - 13653/T) \quad (5.19)$$

$$K_{Wa} = \exp(-16.16 + 6636/T) \quad (5.20)$$

The values of the activation energy of the reactions in Eq. (5.1) and Eq. (5.2) are 18 and 122 kJ/mol from the concentration-based model, respectively, and 19 and 114 kJ/mol from the activity-based model, respectively. The enthalpy of water adsorption is 56 and 55 kJ/mol from the concentration-based model and the activity-based model, respectively.

.

5.4 Permeation study

Assuming that partial pressure of all species in the permeate side was low, the permeation rate of species *i* through the membrane can be expressed as

$$n_i = AP_i a_i \qquad (5.21)$$

where n_i represents the permeation rate of species *i* through the membrane.
A and P_i are the area of membrane and the permeability coefficient of species *i*, respectively.

The relationship between the permeability coefficient and operating temperature can be expressed by Arrhenius' equation

$$P = P_0 \exp\left(\frac{-E_a}{R_g T}\right) \qquad (5.22)$$

where P_o is the pre-exponential factor, E_a the activation energy of permeation, R_g the gas constant, and T the absolute temperature.

The permeation studies of EtOH-H_2O binary mixtures were carried out at a constant temperature of 343 K. Table 5.1 summarizes the feed activity, permeation flux, permeability coefficients of H_2O and EtOH and separation factor at various feed compositions. The separation factor was defined as the ratio of the permeability coefficient of H_2O divided by that of EtOH. The mole fraction of H_2O was varied from 27.7 to 83.0 mol%. It was observed that the activities of H_2O and EtOH were significantly different from the ideality. The permeability coefficient of H_2O was around 100 times higher than that of EtOH at rich contents of EtOH. However, at H_2O content of greater than 62mol%, the decreased H_2O permeability coefficient while the increased EtOH permeability coefficient were observed, resulting in lower separation factor. The inferior performance may be due to the swelling and coupling effect: i.e. the crosslink was destroyed at high H_2O content (Svetlana *et al.*, 1997). However, the H_2O content from this reaction system was much lower than this observed value and, consequently, the membrane degradation did not occur in this study.

Another set of experiment was carried out using quaternary system (H_2O-EtOH-TBA-ETBE). The results at the temperature of 343 K were summarized in

Table 5.2. It was found that the H_2O permeability coefficient was much higher than the other components. The average values of P_{H2O}, P_{EtOH} and P_{TBA} were 6.01×10^{-3}, 8.80×10^{-5} and 1.89×10^{-5} mol/(m^2s), respectively. It should be noted that the permeability coefficients were slightly deviated with feed compositions. This may be due to the interaction between the components. However, to simplify the model, this effect was neglected in this study. More accurate model should be investigated in future studies.

Figure 5.10 shows the Arrhenius plot of the permeability coefficients which can be expressed by the following equations

$$P_{H2O} = \exp(2.07 - 2441 / T) \quad (5.23)$$

$$P_{EtOH} = \exp(3.25 - 4328 / T) \quad (5.24)$$

$$P_{TBA} = \exp(7.67 - 6434 / T) \quad (5.25)$$

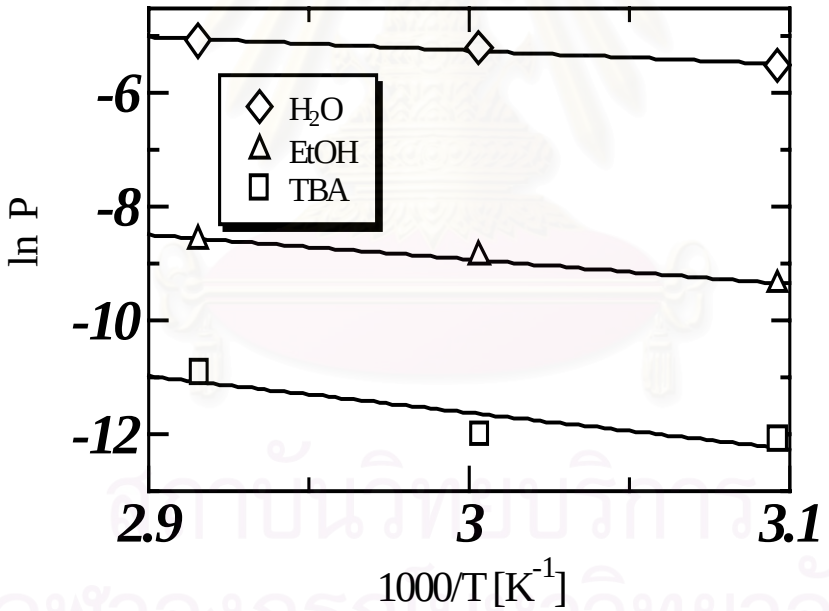

Figure 5.10 Arrhenius plot.

Table 5.1 Permeate fluxes, permeability coefficients and separation factor for binary mixtures at 343 K

Feed composition (mole fraction)		Feed activity		Permeate flux [mol/(m^2.s)]		Permeability coefficient , P_i [mol/(m^2.s)]		Separation factor
H_2O	EtOH	H_2O	EtOH	H_2O	EtOH	H_2O	EtOH	
0.277	0.723	0.516	0.767	3.47×10^{-3}	5.42×10^{-5}	6.72×10^{-3}	7.07×10^{-5}	95
0.345	0.655	0.598	0.718	4.35×10^{-3}	4.91×10^{-5}	7.26×10^{-3}	6.84×10^{-5}	106
0.381	0.619	0.638	0.692	4.59×10^{-3}	3.85×10^{-5}	7.20×10^{-3}	5.56×10^{-5}	129
0.475	0.525	0.724	0.625	5.12×10^{-3}	4.11×10^{-5}	7.06×10^{-3}	5.57×10^{-5}	108
0.620	0.380	0.820	0.543	4.60×10^{-3}	3.83×10^{-5}	5.61×10^{-3}	7.06×10^{-5}	79
0.767	0.233	0.883	0.460	2.64×10^{-3}	5.78×10^{-5}	2.99×10^{-3}	1.26×10^{-4}	24
0.830	0.170	0.905	0.416	2.80×10^{-3}	5.13×10^{-5}	3.10×10^{-3}	1.23×10^{-4}	25

Table 5.2 Permeate fluxes and permeability coefficients of quaternary mixtures at 343 K

Feed composition (mole fraction)				Feed activity				Permeate flux [mol/(m^2.s)]				Permeability coefficient , P_i [mol/(m^2.s)]			
H_2O	EtOH	TBA	ETBE	H_2O	EtOH	TBA	ETBE	H_2O	EtOH	TBA	ETBE	H_2O	EtOH	TBA	ETBE
0.092	0.437	0.435	0.036	0.246	0.445	0.447	0.081	1.30×10^{-3}	3.77×10^{-5}	9.56×10^{-6}	0	5.28×10^{-3}	8.48×10^{-5}	2.14×10^{-5}	0
0.144	0.412	0.380	0.064	0.353	0.425	0.398	0.136	2.10×10^{-3}	3.70×10^{-5}	9.32×10^{-6}	0	5.95×10^{-3}	8.72×10^{-5}	2.34×10^{-5}	0
0.146	0.440	0.343	0.070	0.353	0.455	0.360	0.151	2.21×10^{-3}	3.98×10^{-5}	6.59×10^{-6}	0	6.26×10^{-3}	8.75×10^{-5}	1.83×10^{-5}	0
0.183	0.408	0.348	0.062	0.432	0.421	0.370	0.130	2.75×10^{-3}	3.86×10^{-5}	6.17×10^{-6}	0	6.35×10^{-3}	9.17×10^{-5}	1.67×10^{-5}	0
0.231	0.422	0.267	0.080	0.517	0.439	0.290	0.172	3.21×10^{-3}	3.90×10^{-5}	4.26×10^{-6}	0	6.20×10^{-3}	8.88×10^{-5}	1.47×10^{-5}	0
									average			6.01×10^{-3}	8.80×10^{-5}	1.89×10^{-5}	0

5.5 Pervaporative membrane reactor

The pervaporative membrane reactor was carried out under semi-batch operation. Water in the reaction mixture was simultaneously removed from the system by the pervaporation process while the reaction proceeded. By performing the material balance for the pervaporative membrane reactor, the following expressions are obtained.

$$\frac{d}{dt} m_{TBA} = -n_{TBA} - W(r_1 + r_2) \quad (5.26)$$

$$\frac{d}{dt} m_{H_2O} = -n_{H_2O} + W(r_1 + r_2) \quad (5.27)$$

$$\frac{d}{dt} m_{EtOH} = -n_{EtOH} - Wr_1 \quad (5.28)$$

$$\frac{d}{dt} m_{ETBE} = -n_{ETBE} + Wr_1 \quad (5.29)$$

Figures 5.11, 5.12 and 5.13 show typical results of the concentration profiles of H_2O, EtOH, TBA and ETBE at T = 323, 333 and 343 K, respectively. The concentration presented in mol/kg was determined by using mole fraction and molecular weight of each component. The initial moles of each species were given in the figure captions. It can be seen that the production of ETBE became higher with the increase of temperature. The continuous lines represent the simulation results by using Eqs. (5.8)-(5.9), (5.14) and (5.18)-(5.29). It was observed that the simulation results agreed well with the experimental results.

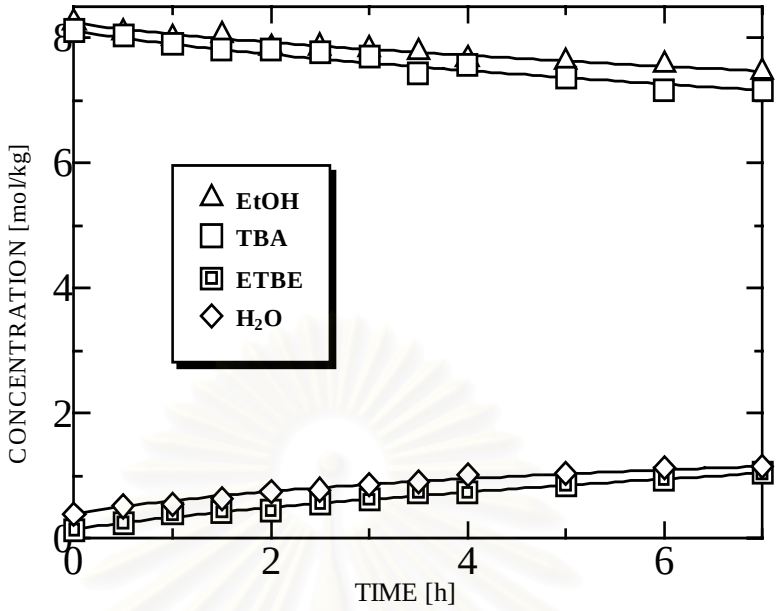

Figure 5.11 Concentration profiles with reaction time (β-zeolite catalyst weight = 15 g, $m_{TBA,o}$ = 1.92 mol, $m_{EtOH,o}$ = 1.95 mol, $m_{ETBE,o}$ = 0.03 mol, $m_{H_2O,o}$ = 0.09 mol, A = 0.0054 m^2 and T = 323 K).

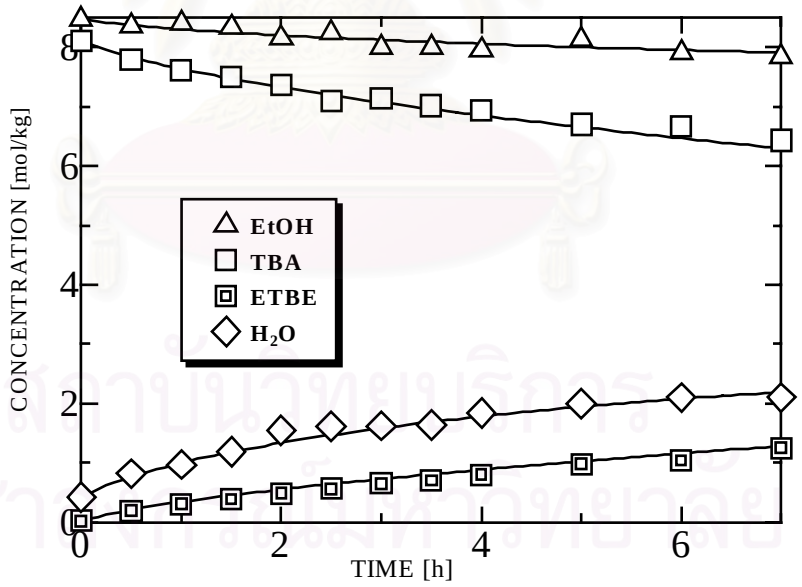

Figure 5.12 Concentration profiles with reaction time (β-zeolite catalyst weight = 15 g, $m_{TBA,o}$ = 1.90 mol, $m_{EtOH,o}$ = 1.99 mol, $m_{ETBE,o}$ = 0.01 mol, $m_{H_2O,o}$ = 0.10 mol, A = 0.0054 $m^2$and T = 333 K).

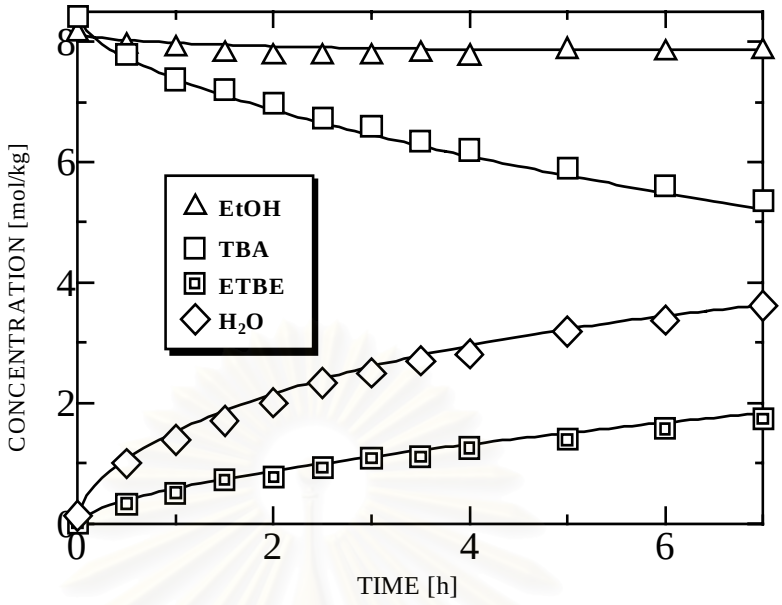

Figure 5.13 Concentration profiles with reaction time (β-zeolite catalyst weight = 15 g, $m_{TBA,o}$ = 2.02 mol, $m_{EtOH,o}$ = 1.95 mol, $m_{ETBE,o}$ = 0 mol, $m_{H_2O,o}$ = 0.03 mol, A = 0.0054 $m^2$and T = 343 K).

5.6 Simulation studies

Figure 5.14 shows the effect of the amount of EtOH on the performance of the conventional reactor without membrane from simulation. α is defined as follow

$$\alpha = \frac{m_{EtOH,0}}{m_{TBA,0}} \qquad (5.30)$$

The increased α increases the selectivity and yield of ETBE. Since TBA can be converted to IB and ETBE, the selectivity of ETBE increases because the forward reaction to ETBE becomes more favorable at higher amount of EtOH.

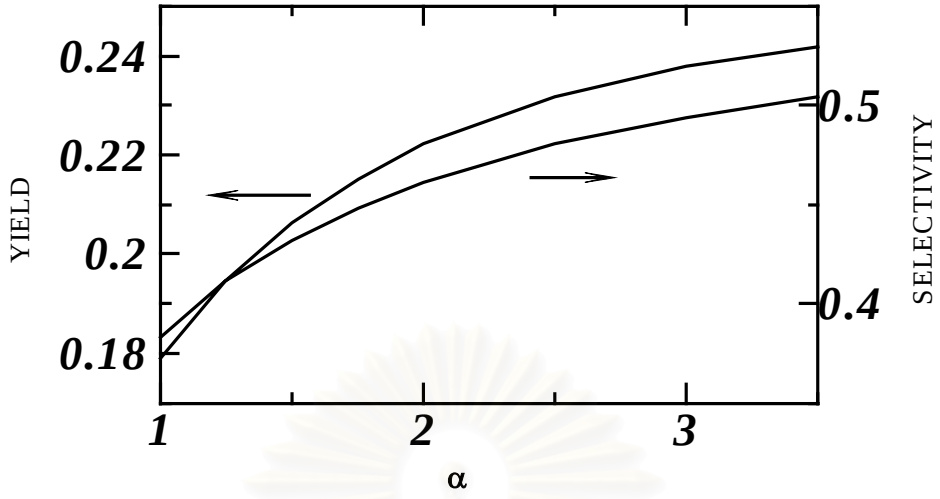

Figure 5.14 The effect of the ratio of initial mole of EtOH to TBA (α) on yield and selectivity (β-zeolite catalyst weight = 15 g, $m_{TBA,o}$ = 2.0 mol, $m_{ETBE,o}$ = 0 mol, $m_{H_2O,o}$ = 0 mol, T = 343 K and reaction time = 7 h).

Figure 5.15 shows the effect of the ratio of membrane area to initial mole of TBA (δ) on the profile of ETBE yield.

$$\delta = \frac{A}{m_{TBA,0}} \qquad (5.31)$$

The case with δ = 0 represents the conventional semi-batch reactor without the membrane. It was observed that the yield increased with the reaction time and that the use of membrane did not only improve the yield but also increase the reaction rate due to the suppressed backward reaction from H_2O removal. The empty and filled symbols represent the experimental results of the cases with δ = 0 and 0.0027 m^2/mol, respectively.

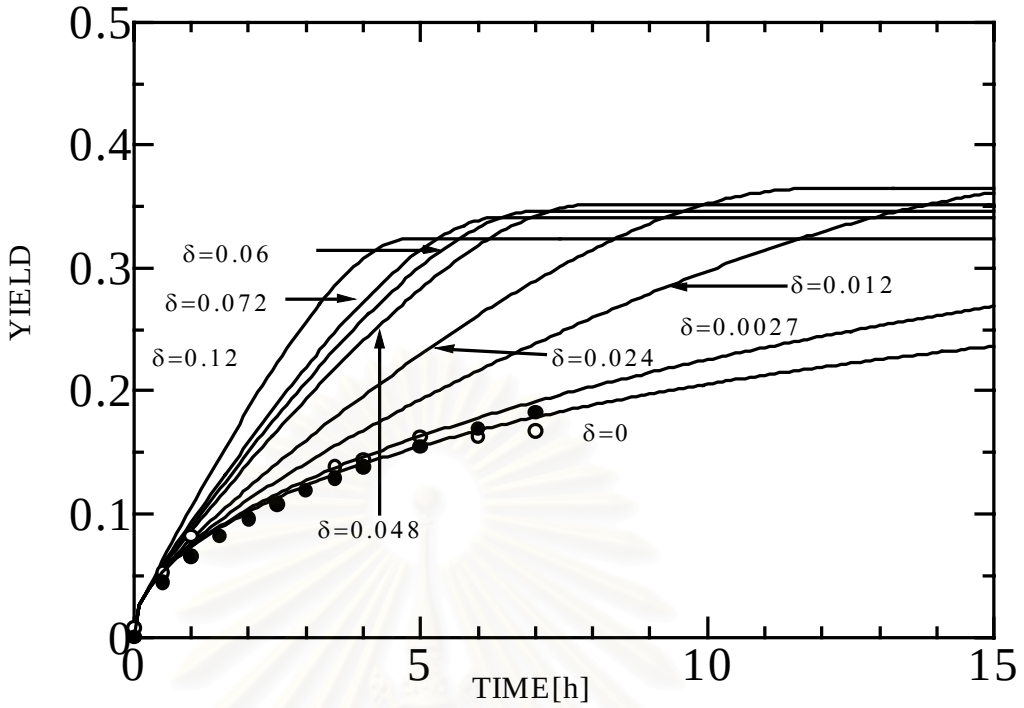

Figure 5.15 The ETBE yield changes during the reaction at different ratios of membrane area to initial mole of TBA (δ) (β-zeolite catalyst weight = 15 g, α = 1.00, $m_{TBA,o}$ = 2.0 mol, $m_{ETBE,o}$ = 0 mol, $m_{H_2O,o}$ = 0 mol and T = 343 K).

However, it is noted that the maximum yield decreased with the increasing δ ratio. This is due to the high EtOH loss with increasing membrane area as shown in Figure 5.16.

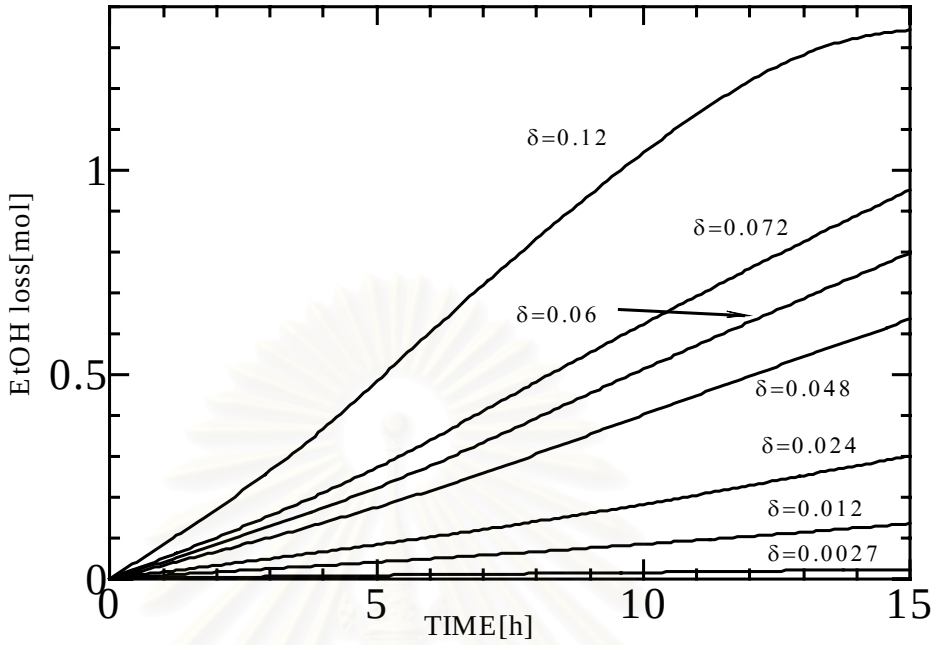

Figure 5.16 The effect of the ratio of membrane area to initial mole of TBA (δ) on the loss of EtOH (β-zeolite catalyst weight = 15 g, α = 1.00, $m_{TBA,o}$ = 2.0 mol, $m_{ETBE,o}$ = 0 mol, $m_{H_2O,o}$ = 0 mol and T = 343 K).

Figure 5.17 shows the effect of the operating temperature on the ETBE yield at various values of δ. The reaction time was fixed at 7 h. It was observed that the ETBE yield increased with increasing temperature. However, at high values of δ, there presented an optimum temperature. The operating temperature directly affected both the reaction rate and the permeation rate of H_2O and the reactants. Increasing reaction rate and the H_2O permeation tended to improve the ETBE yield; however, the reactant loss tended to lower the yield. At high surface area, the effect of reactant loss predominated especially at high temperature since the values of the activation energy of TBA and EtOH were higher than that of H_2O.

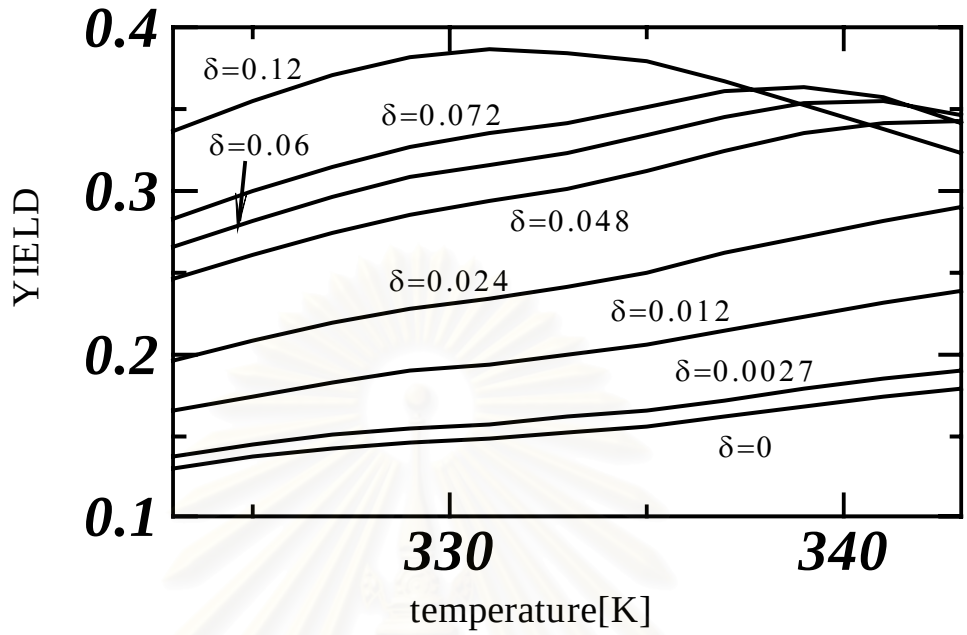

Figure 5.17 The effect of temperature at different ratios of membrane area to initial mole of TBA (δ) on the ETBE yield (β-zeolite catalyst weight = 15 g, α = 1.00, $m_{TBA,o}$ = 2.0 mol, $m_{ETBE,o}$ = 0 mol, $m_{H_2O,o}$ = 0 mol and reaction time = 7 h).

Figure 5.18 shows the effect of the ratio of the amount of catalyst to initial mole of TBA (ϕ) on the ETBE yield. The filled symbol represent the yield at ϕ = 7.5 g/mol.

$$\phi = \frac{W}{m_{TBA,0}} \qquad (5.32)$$

Increasing the ratio of the amount of catalyst to initial mole of TBA (ϕ), increases the ETBE yield. From the above studies, it was clear that the selection of the ratio of initial mole of EtOH to TBA (α), the ratio of membrane area to initial mole of TBA (δ), the ratio of the amount of catalyst to initial mole of TBA (ϕ) and temperature are the key parameters determining the performance of the pervaporative membrane reactor.

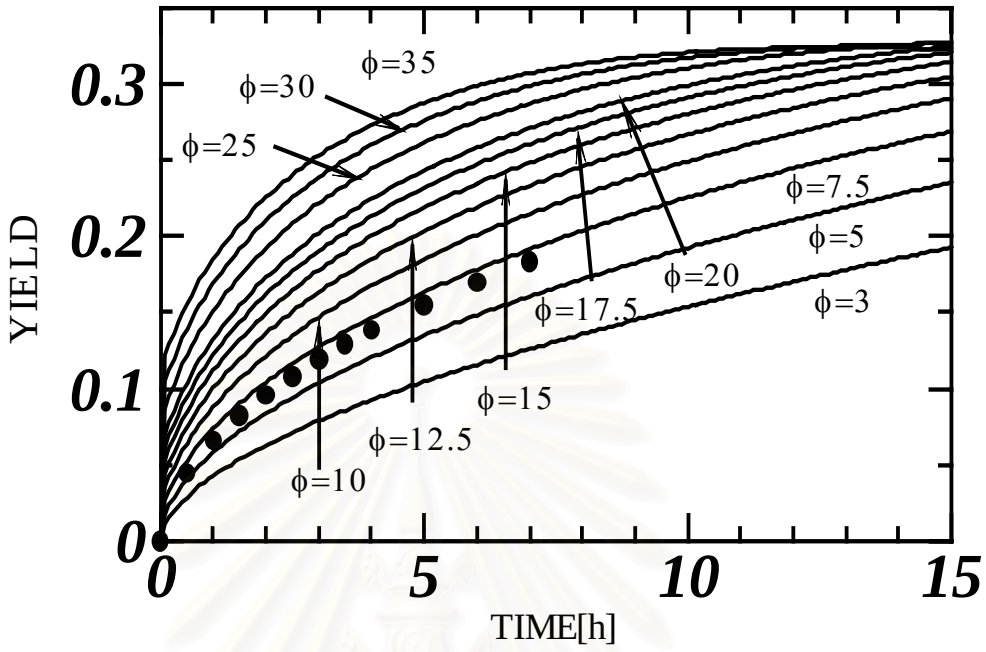

Figure 5.18 The ETBE yield changes during the reaction at different ratios of the amount of catalyst to initial mole of TBA (ϕ) (α = 1.00, $m_{TBA,o}$ = 2.0 mol, $m_{ETBE,o}$ = 0 mol, $m_{H_2O,o}$ = 0 mol, δ = 0 and T = 343 K).

CHAPTER VI

CONCLUSIONS AND RECOMMENDATIONS

Conclusions

Etherification of ethyl *tert*-butyl ether (ETBE) from ethanol (EtOH) and *tert*-butyl alcohol (TBA) was studied in this reseach. The following conclusions can be drawn from the investigation.

1. Kinetic study

1.1 β-Zeolite is an attractive catalyst because β-zeolite showed superior performance over the commercial Amberlyst-15 for the production of ETBE from TBA and EtOH. Even though the activity was moderate, the selectivity was much higher.

1.2 The effect of external mass transfer was constant at the stirring speed higher than 1210 rpm.

1.3 The Arrhenius' equation showed the reaction rate constants, k_{10} and k_{20}, as follows:

Concentration-based model:

$$k_{1c} = \exp(-15.48 - 2186/T)$$

$$k_{2c} = \exp(34.47 - 14688/T)$$

Activity-based model:

$$k_{1a} = \exp(3.55 - 2286/T)$$

$$k_{2a} = \exp(36.57 - 13653/T)$$

1.4 The Van't Hoff equation showed the water inhibition coefficient, K_w

Concentration-based model:

$$K_{Wc} = \exp(-24.72 + 6725/T)$$

Activity-based model:

$$K_{Wa} = \exp(-16.16 + 6636/T)$$

1.5 The values of the activation energy of the ETBE and IB productions were approximately 18 and 122 kJ/mol, respectively.

2. Permeation study

2.1 The permeation studies of H_2O-EtOH binary system using polyvinyl alcohol (PVA) membrane at 343 K revealed that the permeability coefficient of H_2O was around 100 times higher than that of EtOH at rich contents of EtOH.

2.2 The membrane worked effectively for H_2O removal at the mixtures containing H_2O content lower than 62mol%.

2.3 For quaternary system (H_2O-EtOH-TBA-ETBE), the average values of P_{H2O}, P_{EtOH} and P_{TBA} at 343 K were 6.01×10^{-3}, 8.80×10^{-5} and 1.89×10^{-5} mol/(m^2s), respectively. The Arrhenius' equation shows the permeability coefficients, P_i as the following equations

$$P_{H2O} = \exp(2.07 - 2441 / T)$$

$$P_{EtOH} = \exp(3.25 - 4328 / T)$$

$$P_{TBA} = \exp(7.67 - 6434 / T)$$

The values of the activation energy for the permeation of H_2O, EtOH and TBA are 20.3, 36.0 and 53.5 kJ/kmol.

3. Pervaporative membrane reactor study

3.1 Because the product H_2O was simultaneously removed from the reaction zone while the reaction took place in the pervaporative membrane reactor, the performance was superior to the conventional reactors.

3.2 The ratio of initial mole of EtOH to TBA (α), the ratio of membrane area to initial mole of TBA (δ), the ratio of the amount of catalyst to initial mole of TBA (ϕ) and the operating temperature played important roles on the reactor performance.

3.3 The operating temperature and the ratio of membrane area to initial mole of TBA (δ) showed an optimum yield due to the competing effect of rate of reaction and rate of reactant losses.

Recommendations

This work studied the synthesis of ethyl *tert*-butyl ether (ETBE) from ethanol (EtOH) and *tert*-butyl alcohol (TBA) in the pervaporative membrane reactor by performing experiment and computer simulation. However, the experimental results did not show significant improvement over equilibrium conversions. This was because the effective membrane was too small and the driving force enhanced by using inert sweep gas may not be sufficient. It is recommended that using more effective membrane area and a vacuum mode should be employed to emphasize the improvement of reactor performance from the pervaporative membrane reactor concept.

More details on continuous operation of the single or cascade of membrane reactor should be investigated. In addition, a new concept of using two kinds of membranes may be considered. One is the membrane used to remove water in this work and the other is the membrane used to remove the ether as shown in Figure 6.1.

It was observed in this study that the permeability coefficients were slightly deviated with feed compositions. This may be due to the interaction between the components. Therefore, more accurate model should be investigated in future studies.

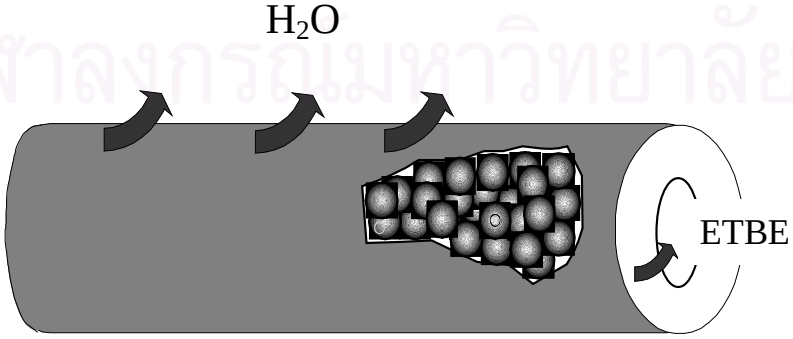

Figure 6.1 Ideal process with two kinds of membranes.

REFERENCES

Ancillotti, F.and V. Fattore. Oxygenate fuels: Market expansion and catalytic aspect of synthesis Fuel Process. Technol. 57(1998) : 163-194.

Cunil, F., M. Vila, J.F. Izquierdo, M. Iborra and J. Tejero. Effect of Water Presence on Methyl *tert*-Butyl Ether and Ethyl *tert*-Butyl Ether Liquid-Phase Synthesis Ind. Eng. Chem. Res. 32(1993) : 564-569.

David, M.O., T.Q. Nguyen and J. Neel. Pervaporation-esterification coupling: PartI.Basic kinetic model. Chem. Eng. Res. Des. 69(1991) : 335-340.

David, M.O., T.Q. Nguyen and J. Neel. Pervaporation-esterification coupling: PartII.Modelling of the influence of different operating parameters. Chem. Eng. Res. Des. 69(1991) : 341-346.

Domingues, L., F. Recasens and M.A.Larrayoz. Studies of a pervaporation reactor: kinetics and equilibrium shift in benzyl alcohol acetylation. Chem. Eng. Sci. 54(1999) : 1461-1465.

Feng, X. and R.Y.M. Huang. Studies of a membrane reactor: esterification facilitated by pervaporation. Chem. Eng. Sci. 51(1996) : 4673-4679.

Fogler, H.S. Elements of Chemical Reaction Engineering . U.S.A. : Prentice Hall, 1992.

Hansen, H.K., P. Rasmussen, Aa. Fredenslund, M. Schiller and J. Gmehling. IEC Research 30(1991) : 2352-2355.

Huang, R.Y.M. Pervaporation membrane separation processes. Netherlands : Elsvier Science, 1991.

Ishigaki, S. and S. Goto. Kinetic studies on liquid-phase hydrogenation of 1-methylnaphthalene using an improved basket reactor. J. Chem. Eng. Jpn. 27 (1994) : 309-313.

Jensen, K.L. and R. Datta. Ethers from ethanol.1.Equilibrium thermodynamic analysis of the liquid-phase ethyl *tert*-butyl ether reaction. Ind. Eng. Chem. Res. 34 (1995) : 392-399.

Keurentjes, J.T.F., G.H.R. Janssen and J.J. Gorissen. The esterification of tartaric acid with ethanol: kinetics and shifting the equilibrium by means of pervaporation. Chem. Eng. Sci. 49(1994) : 4681-4689.

Kita, H., S. Sasaki, K. Tanaka, K. Okamoto and M. Yamamoto.Esterification of carboxylic acid with ethanol accompanied by membrane separation. Chem. Lett. (1988) : 2025-2028.

Kita, H., K. Tanaka, K. Okamoto and M. Yamamoto. The esterification of oleic acid with ethanol accompanied by membrane separation. Chem. Lett. (1987) : 2053-2056.

Krupiczka, R. and Z. Koszorz. Activity-based model of the hybrid process of an esterification reaction coupled with pervaporation. Sep. Puri. Tech. 16(1999) : 55-59.

Lee, C.H. and W.H. Hong. Influence of different degrees of hydrolysis of poly(vinyl alcohol) membrane on transport properties in pervaporation of IPA/water mixture. J.Mem.Sci. 135(1997) : 187-193.

Luo, G.S., M. Niang and P. Schaetzel. Separation of ethyl tert-butyl ether-ethanol by combined pervaporation and distillation. Chem. Eng. J. 68(1997) : 139-143.

Matouq, M., A. Quitain, K. Takahashi and S. Goto. Reactive distillation for synthesizing ethyl *tert*-butyl ether from low-grade alcohol catalyzed by potassium hydrogeb sulfate. Ind. Eng. Chem. Res. 35(1996) : 982-984.

Matouq, M., T. Tagawa and S. Goto. Combined process for production of methyl tert-butyl ether from tert-butyl alcohol and methanol. J. Chem. Eng. Jpn. 27(1994) : 302-306.

Okamoto, K., M.Yamamoto, Y.Otoshi, T.Semoto, M.Yano, K.Tanaka and H.Kita. Pervaporation-aided esterification of oleic acid. J. Chem. Eng. Jpn. 26(1993) : 475-481.

Oudshoorn, O.L., M. Janissen, W.E.J. van Kooten, J.C. Jansen, H. van Bekkum, C.M. van den Bleek, H.P.A. Calis. A novel structured catalyst packing for catalytic distillation of ETBE. Chem. Eng. Sci. 54(1999) :1413-1418.

Parkinson, G. All side pumped up for MTBE ban. Chem.Eng-NEW YORK 106 (June 1999) : 49.

Panichsarn, S., S. Phaitanasri, P. Praserthdam, T. Mongkhonsri. Cumene Synthesis from Benzene and Isopropanol Over Beta Zeolite. Master of Engineering thesis, Department of Chemical Engineering, Faculty of Engineering Chulalongkorn University, 1999.

Quitain, A., H. Itoh, S. Goto. Industrial-scale simulation of proposed process for synthesizing ethyl *tert*-butyl ether from bioehanol J. Chem. Eng. Jpn. 32(1999) : 539-543.

Quitain, A., H. Itoh, S. Goto. Reactive distillation for synthesizing ethyl *tert*-butyl ether from bioehanol. J. Chem. Eng. Jpn. 32(1999) : 280-287.

Ramesh B. Borade and A. Clearfield. Characterization of acid sites in Beta and ZSM-20 zeolites. J.Phys.Chem. 96(1992) : 6729-6737.

Rihko, L.K. and A.O. Krause. Etherification of FCC light gasoline with methanol. Ind. Eng. Chem.Res. 35(1996) : 2500-2507.

Sentarh, I., S. Dincer and O. Tunc Savasci. Pervaporation separation of methanol-carbontetrachloride binary mixtures using low density polyethylene membranes. Chem.Eng.Tech. 21(1998) : 359-364.

Svetlana, I., O. Haruhiko and S. Khantong. Hydrophilic membrane for pervaporation: An analytical review. Desalination. 110(1997) : 251-286.

Tungudomwongsa, H., T. Mongkhonsi, P. Praserthdam, S. Phatanasri. Development of Alumina Coating on a Ceramic Monolith. Master of Engineering thesis, Department of Chemical Engineering, Faculty of Engineering Chulalongkorn University, 1997.

Waldburger, R., F. Widmer and W. Heinzelmann. Combination of esterification and pervaporation in a continuous membrane reactor. Chem. Ing. Tech. 66(1994) : 850-854.

Yang, B. and S. Goto. Pervaporation with reactive distillation for the production of ethyl *tert*-butyl ether. Sep. Sci. Tech. 32(1997) : 971-981.

Yang, B., S.B. Yang and R.Q. Yao. Synthesis of Ethyl *tert*-Butyl Ether from *tert*-butyl alcohol and ethanol on strong acid cation-exchange resins. React. Funct. Polym. 44(2000) : 167-175.

Yin, X., B. Yang and S. Goto. Kinetics of liquid-phase synthesis of ethyl *tert*-butyl ether from *tert*-butyl alcohol and ethanol catalyzed by ion-exchange resin and heteropoly acid. Int. J. Chem. Kinet. 27(1995) : 1065-1074.

Zhu, Y., G. Minet and T.T. Tsotsis. A continuous pervaporation membrane reactor for the study of esterification reactions using composite polymeric/ceramic membrane. Chem. Eng. Sci. 51(1996) : 4103-4113.

APPENDICES

APPENDIX A

CORRECTION FACTOR

Correction faction for a gas chromatography (GC) with column Gaskuropack 54

Correction faction, $F_i = \frac{(\Theta_i / m_i)}{(\Theta / m)_{STANDARD}}$ (A-1)

Given methyl *tert*-butyl ether (MTBE) is standard component ($F_{MTBE} = 1$)

REACTANTS	MOLE (m_i)	AREA (Θ_i)	CORRECTION FACTOR (F_i)
H_2O	2.187×10^{-8}	318420	0.3266
EtOH	6.630×10^{-9}	215674	0.7297
TBA	4.135×10^{-9}	171234	0.9289
MTBE	3.585×10^{-9}	159814	1.0000
ETBE	3.039×10^{-9}	130855	0.9659

APPENDIX B

CALCULATION OF NUMBER OF MOLE

Number of mole of each component can calculate by using correction factors from Appendix A.

$$m_i = x_i \text{ x } m_{total} \qquad \text{(B-1)}$$

where m_i and m_{total} are the number of mole of species *i* and total mole, respectively.

x_i represents mole fraction of component.

$$x_i = \frac{\Theta_i / F_i}{\Sigma(\Theta_i / F_i)} \qquad \text{(B-2)}$$

For example; Batch reactor

Reaction condition; temperature = 343 K, stirring speed = 1210 rpm, β-zeolite catalyst weight = 15 g and total mole = 4 mole.

REACTANTS	AREA	CORRECTION FACTOR(F)	MOLE FRACTION	NUMBER OF MOLE
H_2O	20885	0.3266	0.0254	0.1016
EtOH	908761	0.7297	0.4949	1.9797
TBA	1113322	0.9289	0.4763	1.9051
ETBE	8248	0.9659	0.0034	0.0136

APPENDIX C

UNIFAC CALCULATION

The UNIQUAC equation treats $g \equiv G^E / RT$ as comprised of two additive parts, a *combinatorial* term g^C to account for molecular size and shape differences, and a *residual* term g^R to account for molecular interactions:

$$g = g^C + g^R \tag{C-1}$$

Function g^C contains pure-species parameters only, whereas function g^R incorporates two binary parameters for each pair of molecules. For a multicomponent system,

$$g^C = \sum x_i \ln \frac{\phi_i}{x_i} + 5 \sum q_i x_i \ln \frac{\theta_i}{\phi_i} \tag{C-2}$$

and

$$g^R = -\sum q_i x_i \ln(\sum \theta_j \tau_{ji}) \tag{C-3}$$

where

$$\phi_i = \frac{x_i r_i}{x_j r_j}_i \tag{C-4}$$

and

$$\theta_i = \frac{x_i q_i}{x_j q_j}_i \tag{C-5}$$

Subscript i identifies species, and j is a dummy index; all summations are over all species. Note that $\tau_{ji} \neq \tau_{ii}$; however, when $i = j$, then $\tau_{jj} = \tau_{ii} = 1$. In these equations r_i (a relative molecular volume) and q_i (a relative molecular surface area) are pure-species parameters. The influence of temperature on g enters through the interaction parameters τ_{ji} of Eq.(C-3), which are temperature dependent:

$$\tau_{ji} = exp \frac{-(u_{ji} - u_{ii})}{RT}_i \tag{C-6}$$

Parameters for the UNIQUAC equation are therefore values of $(u_{ji} - u_{ii})$.

An expression for $\ln \gamma_i$ is applied to the UNIQUAC equation for g [Eqs.(C-1) through (C-3)]. The result is given by the following equations:

$$\ln \gamma_i = \ln \gamma_i^C + \ln \gamma_i^R \tag{C-7}$$

$$\ln \gamma_i^C = 1 - J_i + \ln J_i - 5q_i(1 - \frac{J_i}{L_i} + \ln \frac{J_i}{L_i}) \tag{C-8}$$

and $$\ln \gamma_i^{R} = q_i (1 - \ln s_i - \sum \theta_j \frac{\tau_{ij}}{s_j}) \quad \text{(C-9)}$$

where in addition to Eqs. (C-5) and (C-6)

$$J_i = \frac{r_i}{\sum x_j r_j} \quad \text{(C-10)}$$

$$L_i = \frac{q_i}{\sum x_j q_j} \quad \text{(C-11)}$$

$$s_i = \sum \theta_l \tau_{li} \quad \text{(C-12)}$$

Again subscript *i* identifies species, and *j* and *l* are dummy indices. All summations are over all species, and τ_{ij} =1 for *i*=*j*. Values for the parameters (u_{ij} - u_{jj}) are found by regression of binary VLE data, and are given by Gmehling et al.

The UNIFAC method for estimation of activity coefficient depends on the concept that a liquid mixture may be considered a solution of the structural units from which the molecules are formed lather than a solution of the molecules themselves. These structural units are called subgroups, and a few of them are listed in the second column of table C.1. A number, designated k, identifies each subgroup. The relative volume R_k and relative surface area Q_k are properties of the subgroups, and values are listed in column 4 and 5 of Table C.1. Also shown (columns 6 and 7) are examples of the subgroup compositions of molecular species. When it is possible to construct a molecule from more than one set of subgroups, the set containing the least member of different subgroups id the correct set. The great advantage of the UNIFAC method is that a relatively small number of subgroups combine to form a very large number of molecules.

Activity coefficients depend not only on the subgroup properties R_k and Q_k, but also on interactions between subgroups. Here, similar subgroups are assigned to a main group, as shown in the first two columns of Table C.1. The designations of main groups, such as "CH_2" , "ACH", etc., are descriptive only. All subgroups belonging to the same main group are considered identical with respect to group interactions. Therefore parameters characterizing group interactions are identified with pairs of main groups. Parameter value a_{mk} for a few such pairs are given in table C.2.

The UNIFAC method is base on the UNIQUAC equation, for which the activity coefficients are given by equation C-7. When applied to a solution of groups, Eqs. C-8 and C-9 are written:

$$\ln \gamma_i^{\,C} = 1 - J_i + \ln J_i - 5q_i\left(1 - \frac{J_i}{L_i} + \ln \frac{J_i}{L_i}\right) \qquad \text{(C-13)}$$

and

$$\ln \gamma_i^{\,R} = q_i\left[1 - \sum\left(\theta_k \frac{\beta_{ik}}{s_k} - e_{ki} \ln \frac{\beta_{ik}}{s_k}\right)\right] \qquad \text{(C-14)}$$

The quantities J_i and L_i are still given by Eqs. C-10 and C-11. In addition, the following definition apply:

$$r_i = \sum \nu_k^{(i)} R_k \qquad \text{(C-15)}$$

$$q_i = \sum \nu_k^{(i)} Q_k \qquad \text{(C-16)}$$

$$e_{ki} = \frac{\nu_k^{(i)} Q_k}{q_i} \qquad \text{(C-17)}$$

$$\beta_{ik} = \sum e_{mi} \tau_{mk} \qquad \text{(C-18)}$$

$$\theta_k = \frac{\sum x_i q_i e_{ki}}{\sum x_j q_j} \qquad \text{(C-19)}$$

$$s_k = \sum \theta_m \tau_{mk} \qquad \text{(C-20)}$$

$$\tau_{mk} = \exp \frac{-a_{mk}}{T} \qquad \text{(C-21)}$$

Subscript i identifies species, and j is a dummy index running over all species. Subscript k identifies subgroups, and m is a dummy index running over all subgroups. the quantity $\nu_k^{(i)}$ is the number of subgroups of type k in a molecule of species i. Values of the subgroup parameters R_k and Q_k and of the group interaction parameters a_{mk} come from tabulation in the literature. Tables C.1 and C.2 show a few parameter values; the number designations of the compete table are remained.

Table C.1: UNIFAC-VLE subgroup parameters

Main group	Subgroup	k	R_k	Q_k	Examples of molecules and their constituent groups	
1 "CH_2"	CH_3	1	0.9011	0.848	n-Butane:	2 CH_3, 2 CH_3
	CH_2	2	0.6744	0.540	Isobutane:	3 CH_3, 1 CH
	CH	3	0.4469	0.228	2,2-Dimethyl	
	C	4	0.2195	0.000	propane:	4 CH_3, 1 C
3 "ACH" (AC = aromatic carbon)	ACH	10	0.5313	0.400	Benzene	6 ACH
4 "$ACCH_2$"	$ACCH_3$	12	1.2663	0.968	Toluene:	5 ACH, 1 $ACCH_3$
	$ACCH_2$	13	1.0396	0.660	Ethylbenzene:	1CH_3, 5ACH, 1 $ACCH_2$
5 "OH"	OH	15	1.0000	1.200	Ethanol:	1 CH_3, 1 CH_2, 1 OH
7 "H_2O"	H_2O	17	0.9200	1.400	Water:	1 H_2O
9 "CH_2CO"	CH_3CO	19	1.6724	1.488	Acetone:	1 CH_3CO, 1 CH_3
	CH_2CO	20	1.4457	1.180	3-Pentanone:	2 CH_3, 1 CH_2CO, 1 CH_2
13 "CH_2O"	CH_3O	25	1.1450	1.088	Dimethyl ether:	1 CH_3, 1 CH_3O
	CH_2O	26	0.9183	0.780	Diethyl ether:	2 CH_3, 1 CH_2, 1 CH_2O
	CH-O	27	0.6908	0.468	Diisopropyl	
					ether:	4 CH_3, 1CH, 1 CH-O
15 "CNH"	CH_3NH	32	1.4337	1.244	Dimethylamine:	1 CH_3, 1 CH_3NH
	CH_2NH	33	1.2070	0.936	Diethylamine:	2 CH_3, 1 CH_2, 1 CH_2NH
	CHNH	34	0.9795	0.624	Diisopropyl	
					amine:	4 CH_3, 1 CH, 1 CHNH
19 "CCN"	CH_3CN	41	1.8701	1.724	Acetonitrile:	1 CH_3CN
	CH_2CN	42	1.6434	1.416	Propionitrile:	1CH_3, 1 CH_2CN

Table C.2: UNIFAC-VLE interaction parameters, a_{mk}, in kelvins

	1	3	4	5	7	9	13	15	19
1 CH_2	0.00	61.13	76.50	986.50	1,318.0	476.40	251.50	255.70	597.00
3 ACH	-11.12	0.00	167.00	636.10	903.80	25.77	32.14	122.80	212.50
4 $ACCH_2$	-69.70	-146.80	0.00	803.20	5,695.0	-52.10	213.10	-49.29	6,096.0
5 OH	156.40	89.60	25.82	0.00	353.50	84.00	28.06	42.70	6.712
7 H_2O	300.00	362.30	377.60	-229.10	0.00	-195.40	540.50	168.00	112.60
9 CH_2CO	26.76	140.10	366.80	164.50	472.50	0.00	-103.60	-174.20	481.70
13 CH_2O	83.36	52.13	65.69	237.70	-314.70	191.10	0.00	251.50	-18.51
15 CNH	65.33	-22.31	223.00	-150.00	-448.20	394.60	-56.08	0.00	147.10
19 CCN	24.82	-22.97	-138.40	185.40	242.80	-287.50	38.81	-108.50	0.00

In a liquid phase reaction between EtOH and TBA to form ETBE and H_2O, the subgroups of each species were performed following.

EtOH : 1 CH_3, 1 CH_2, 1 OH

TBA : 3 CH_3, 1 C, 1 OH

ETBE : 4 CH_3, 1 C, 1 CH_2O

H_2O : 1 H_2O

The parameters using in UNIFAC calculation were summarized as follows.

UNIFAC-VLE subgroup parameters

Main Group	Subgroup	k	R_k	Q_k
1 "CH_2"	CH_3	1	0.9011	0.848
	CH_2	2	0.6744	0.540
	C	4	0.2195	0.000
5 "OH"	OH	15	1.0000	1.200
7 "H_2O"	H_2O	17	0.9200	1.400
13 "CH_2O"	CH_2O	26	0.9183	0.780

UNIFAC-VLE interaction parameters, a_{mk}, in kelvins

	1	5	7	13
1 CH_2	0.00	986.50	1,318.00	251.50
5 OH	156.40	0.00	353.50	28.06
7 H_2O	300.00	-229.10	0.00	540.50
13 CH_2O	83.36	237.70	-314.70	0.00

APPENDIX D

MEMBRANE PROPERTIES

Polyvinyl alcohol (PVA) membranes (PERVAP 2201) supplied by Sulzer Chemtech GmbH-Membrane Systems were used as a hydrophilic membrane. The properties were described as followings.

Code	PERVAP 2201
Main Application	Neutral solvents Reaction mixtures
Max. Temperature Long Term,°C	100
Max. Temperature Short Term,°C	105
Max. Water Content in Feed, %b.w.	≤ 90
Major Limitation	
Aprotic Solvents (e.g. DMF, DMSO)	≤ 1 %
Organic Acids (e.g. acetic acid)	≤ 50 %
Formic Acid	≤ 0.5 %
Mineral Acids (e.g. H_2SO_4)	≤ 1 %
Alkali (e.g. NaOH)	≤ 10 ppm
Aliphatic Amines (e.g. Triethylamin)	≤ 50 %
Aromatic Amines (e.g. Pyridine)	≤ 50 %

VITA

Mr. Worapon Kiatkittipong was born in May 29, 1978 in Phichit, Thailand. He finished high school from Bodindecha (Sing Singhasaenee) School, Bangkok in 1995. He received his Bachelor's Degree in Chemical Engineering, from the Department of Chemical Engineering, Faculty of Engineering, Kasetsart University, Bangkok in 1999.